E&G Quaternary Sci. J., 69, 165–186, 2020
https://doi.org/10.5194/egqsj-69-165-2020

Open Access E&G Quaternary Science Journal

Research article

Reconstruction of palaeoenvironmental variability based on an inter-comparison of four lacustrine archives on the Peloponnese (Greece) for the last 5000 years

Joana Seguin[1], Pavlos Avramidis[2], Annette Haug[3], Torben Kessler[3], Arndt Schimmelmann[4], and Ingmar Unkel[1]

[1]Institute for Ecosystem Research, Kiel University, Olshausenstraße 75, 24118 Kiel, Germany
[2]Department of Geology, University of Patras, Rio 26504 Patras, Greece
[3]Institute for Classical Archaeology, Kiel University, Johanna-Mestorf-Str. 5, 24118 Kiel, Germany
[4]Department of Earth and Atmospheric Sciences, Indiana University, 1001 E 10th Street, Bloomington, IN 47405-1405, USA

Correspondence: Joana Seguin (jseguin@ecology.uni-kiel.de)

Relevant dates: Received: 2 October 2019 – Revised: 15 July 2020 – Accepted: 3 August 2020 – Published: 13 October 2020

How to cite: Seguin, J., Avramidis, P., Haug, A., Kessler, T., Schimmelmann, A., and Unkel, I.: Reconstruction of palaeoenvironmental variability based on an inter-comparison of four lacustrine archives on the Peloponnese (Greece) for the last 5000 years, E&G Quaternary Sci. J., 69, 165–186, https://doi.org/10.5194/egqsj-69-165-2020, 2020.

Abstract: A high quantity of well-dated, high-resolution, continuous geoarchives is needed to connect palaeoenvironmental reconstructions with socio-environmental and cultural transformations in a geographically heterogeneous region such as southern Greece. However, detailed and continuous palaeoclimatic and palaeoenvironmental archives from the NE Peloponnese are still sparse. Here, we present two new palaeolake archives of Pheneos and Kaisari covering the last 10 500 and 6500 years, respectively. For the last 5000 years, we compare them with sediment records from adjacent Lake Stymphalia and the Asea valley by applying the same set of sedimentological, geochemical, and statistical analyses to all four lacustrine archives.

Continuous geochemical X-ray fluorescence (XRF) core scanning records provide evidence for hydrological variations and environmental changes since the Early Helladic period (5050 BP), the beginning of the Bronze Age in Greece. We hereby focus on different spatial scales to estimate the validity range of the proxy signals. Ten elements were selected (Al, Si, K, Ca, Ti, Mn, Fe, Rb, Sr, Zr) for a principal component analysis. The clr(Ca/Ti) was chosen as the most meaningful proxy, reflecting varying input of carbonaceous vs. clastic input, which may be linked to changes in the hydrological conditions. Our results show phases when permanent lake water bodies existed (ca. 5000–3600 cal BP) as well as phases with periodic desiccation of the lakes during younger times. While Pheneos and Kaisari show a drying trend during the transition phase from the Late Helladic period to the Proto-Geometric period (ca. 3200–2800 cal BP), Stymphalia and Asea show a rather short dry peak around 3200 cal BP followed by a wetter phase.

Although all our geoarchives show evidence for drier phases, their timing and duration display considerable site-to-site differences which may be explained by site-specific responses in individual ecosystems. Age uncertainties, however, may likewise explain some deviations, as the dating is based on bulk sediment samples including potential unknown reservoir effects.

Published by Copernicus Publications on behalf of the Deutsche Quartärvereinigung (DEUQUA) e.V.

The high regional geographical diversity within the Peloponnese combined with the dating challenges in the limestone-rich area and the variation in our data testify that any hypothetical mono-causal connection between palaeoenvironmental changes in a single geoarchive and contemporaneous societal transformations across the Peloponnese would be an oversimplification.

Kurzfassung:

Eine hohe Anzahl gut datierter, hochaufgelöster und kontinuierlicher Geoarchive wird benötigt, um Paläoumweltrekonstruktionen mit sozial-ökologischen und kulturellen Transformationen in einer geographisch heterogenen Region wie Südgriechenland zu verknüpfen. Aktuell sind solch detaillierte und durchgängige Paläoklima- sowie Paläoumweltarchive auf der NO Peloponnes jedoch spärlich.

In dieser Arbeit stellen wir kontinuierliche Proxydaten für zwei neue Umweltarchive aus den Paläoseen Pheneos und Kaisari vor, welche die letzten 10 500 bzw. 6500 Jahre abdecken. Für den Zeitraum der letzten 5000 Jahre vergleichen wir diese mit Sedimentkernen des angrenzenden Sees Symphalia sowie des Asea Tals, indem wir für alle vier lakustrinen Archive die gleichen sedimentologischen, geochemischen und statistischen Analysen durchführen.

Röntgenfluoreszenz-Kernscandaten liefern Hinweise auf hydrologische Schwankungen und Umweltveränderungen seit der frühhelladischen Zeit (5050 BP), dem Beginn des Bronzezeitalters in Griechenland. In dieser Arbeit konzentrieren wir uns auf verschiedene räumliche Skalen, um den Gültigkeitsbereich der Proxysignale abzuschätzen. Eine Hauptkomponentenanalyse wurde auf Basis von zehn geochemischen Elementen (Al, Si, K, Ca, Ti, Mn, Fe, Rb, Sr, Zr) durchgeführt. Das zentrierte log-Verhältnis clr(Ca/Ti) wurde als aussagekräftigster Proxy identifiziert, welcher den veränderlichen Eintrag von calciumcarbonathaltigem zu klastischem Material widerspiegelt, der wiederum auf Veränderungen in den hydrologischen Bedingungen zurückgeführt werden kann. Unsere Ergebnisse zeigen Phasen, in denen dauerhafte Seen an den untersuchten Standorten existierten (ca. 5000–3600 cal BP) sowie Phasen – vor allem in jüngerer Zeit – in denen es zu periodischer Austrocknung der Seen kam. Während Pheneos und Kaisari beispielsweise eine Trockenphase während der Übergangszeit der späthelladischen zur protogeometrischen Periode (ca. 3200–2800 cal BP) erkennen lassen, zeigen Stymphalia und Asea eine eher kurze Trockenphase um 3200 cal BP gefolgt von einer längeren feuchteren Phase.

Auch wenn alle untersuchten Geoarchive klare Anzeichen für Trockenphasen liefern, variieren sowohl der Zeitpunkt als auch die Dauer erheblich, was auf standortspezifische Reaktionen der einzelnen Ökosysteme zurückgeführt werden kann. Unsicherheiten in den Altersmodellen können gleichwohl einige Abweichungen erklären, da die Radiokarbondatierungen auf Basis von Gesamtsedimentproben durchgeführt wurden, welche einen potenziellen, unbekannten Reservoireffekt beinhalten können.

Die hohe räumliche Diversität innerhalb der Peloponnes Halbinsel in Kombination mit den Datierungsunsicherheiten in einem kalkhaltigen Karstgebiet und den Schwankungen in den Datensätzen deuten darauf hin, dass das Herstellen monokausaler Verbindungen zwischen Paläoumweltschwankungen in einem einzelnen Geoarchiv und zeitgleichen sozialen Transformationen auf der Peloponnes eine zu starke Vereinfachung der Forschungshypothesen zur Konsequenz hat.

Highlights. Multi-proxy investigation of Middle to Late Holocene hydrological development from four (palaeo)lake sediment sequences.

Proxy signals are discussed on three different spatial scales.

High regional to local variability of palaeoclimatic proxies across the Peloponnese peninsula.

1 Introduction

The eastern Mediterranean can be considered a region of high importance for palaeoenvironmental research, as it experienced a long history of cultural development and human–environment interaction throughout the Middle to Late Holocene (Izdebski et al., 2016; Roberts et al., 2011).

Middle to Late Holocene environmental archives often provide records on palaeoenvironmental changes containing a combination of natural climatic and anthropogenic signals, which are often not easy to disentangle. From southern Greece and the Peloponnese, high-resolution environmental archives covering this time period are still relatively sparse or often discontinuous (Finné et al., 2011; Gogou et al., 2016; Luterbacher et al., 2012, McCormick et al., 2012; Atherden and Hall, 1994; Izdebski et al., 2016; Jahns, 1993).

Lake sediments record climatic changes as well as local catchment-specific processes (Roberts et al., 2008). However, each lake responds differently to global, regional, or local influences, depending on its size and catchment settings (Meyers and Lallier-Vergès, 1999). To distinguish local from regional or even hemispheric climatic signals, a combination of a larger number of geoarchives and an analysis of multiple proxies seems more promising (Finné et al., 2019).

Although there are an increasing number of studies on eastern Mediterranean palaeoenvironmental archives that have been published most recently (Emmanouilidis et al., 2018, 2019; Finné et al., 2017; Katrantsiotis et al., 2018, 2019; Masi et al., 2018; Rothacker et al., 2018), they do not provide a uniform picture of the climatic and environmental changes through the Middle to Late Holocene, and sometimes they are inconsistent with archaeological or historical data (Finné et al., 2019). Most reconstructions of Holocene climatic variations in the Mediterranean are based on one single palaeoenvironmental archive, leading to very heterogeneous and often even divergent results when being compared to each other (Finné et al., 2011; Luterbacher et al., 2012). This calls for the need for not only multi-proxy approaches on one palaeoenvironmental archive, but also multi-archive approaches that use the same methods and proxies at different study sites.

Here, we present a combined approach of four lake sediment archives from the northeastern and central Peloponnese (Greece), namely from Lake Stymphalia and from the valleys of Asea, Pheneos, and Kaisari (Fig. 1), which hosted lakes of different extent in the past. Human presence in the study area is proven since Neolithic times but has been relatively sparse and remains widely unexplored except for the Classical–Hellenistic periods and the last 200 years (Seguin et al., 2019; Walsh et al., 2017). Due to its mountainous topography with elevations of up to 2400 m only a few kilometres away from the coast, the Peloponnese displays a high climatic heterogeneity with significant precipitation and temperature gradients from west to east and from the coast to the mountain ranges. Hence, palaeoclimate records across the Peloponnese are prone to reveal different patterns on a spatially comparatively limited scale (Katrantsiotis et al., 2019).

The concept of spatial scales is a fundamental working technique in physical geography and climatology (Lauer and Bendix, 2006; Wanner, 1986). The scales however are not uniformly used and may differ according to the studied landforms, climate phenomena, and processes. In this study, we distinguish micro-, meso-, and macroscales and define them as follows: (1) the microscale covers local lake catchment-specific signals and processes, (2) the mesoscale describes the regional climate on the NE Peloponnese with an approximate diameter of 10^2 km (Wanner, 1986), and (3) macroscale signals reflect changes on the supra-regional level, here the eastern Mediterranean. Given the proximity of our selected palaeoenvironmental archives to each other and the similar geological and geomorphological setting, we suppose that they experienced similar mesoscale climatic conditions. We investigate each archive with the same geochemical and sedimentological analytical tools, notably XRF core scanning, to reveal the differences and similarities in the proxy records that help us to disentangle local (microscale) from regional (mesoscale) signals. A concordance in the course of the same proxy at the different sites would suggest that the proxy reflects an overarching signal of regional environmental or climatic change (macroscale). If the proxy shows no agreement between the sites, this may hint towards local site-specific effects or a mismatching of the data due to dating uncertainties (Roberts et al., 2016).

Earlier studies on Lake Stymphalia (Heymann et al., 2013; Seguin et al., 2019) showed that the lake reacted sensitively to environmental and hydrological changes as well as to human disturbances, notably during the last 2500 years. A sediment core from the Asea valley provided a record on the hydrological variability in the area of the last 6500 years (Unkel et al., 2014), however in lower resolution than the Stymphalia record.

In this study, we aim to (1) provide geochemical proxies for two new sediment sequences from palaeolakes Pheneos for the last 10 500 years and Kaisari for the last 6500 years and (2) compare the last 5050 years with the same proxies from nearby Stymphalia and Asea to reconstruct and investigate climatic and environmental changes since the beginning of the Helladic period (for references to cultural periods see Table S3 in the Supplement). This is a period when the Greek societies were already sedentary and achieved major advances in social, economic, and technological skills (Bintliff, 2012). By directly juxtaposing records from four sites, we provide a more profound picture of the environmental and climatic history of the Peloponnese, going beyond the capabilities of a climate reconstruction based on a single lake record.

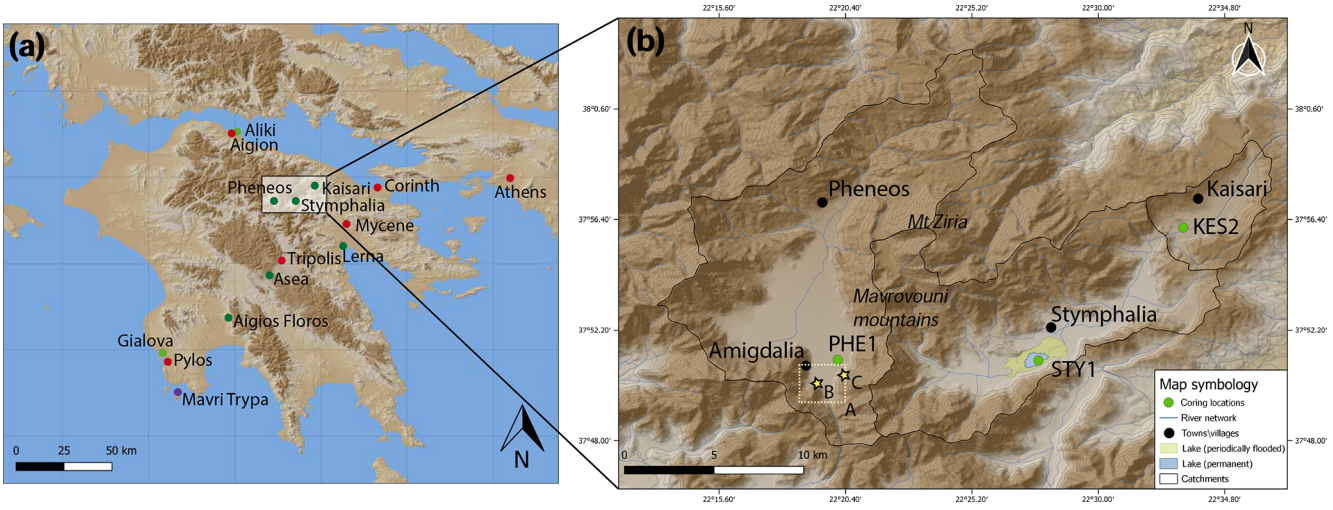

Figure 1. Map of the study area in the NE Peloponnese. **(a)** Overview of the Peloponnese with the location of selected cities and archaeological sites (red), lacustrine (dark green) and lagoonal (light green) sediment archives, and speleothem archives (purple). **(b)** Topographic map of the poljes area with the location of the coring sites (green) and settlements (black). Black lines trace the surface hydrological catchments. Contour lines are drawn in increments of 100 m. Photo locations A–C from Fig. 2 have been indicated by a dotted square and yellow stars.

2 Regional setting

The three karst poljes Pheneos, Stymphalia, and Kaisari are located in the northeastern Peloponnese at the southern base of the Mt. Ziria (also known as Kyllini) (2374 m) limestone massif at an elevation of ca. 600 m above sea level (Fig. 1).

The Stymphalia Polje, extending approximately 13 km from west to east, comprises the only remaining natural permanent lake of the Peloponnese, Lake Stymphalia (37.85° N, 22.46° E), as well as the archaeological site of the Hellenistic town of Stymphalos (Walsh et al., 2017; Williams, 1983; Williams and Gourley, 2005). The total catchment area today is approximately 217 km^2, excluding subsurface water flow of the Ziria karst system (Nanou and Zagana, 2018). The larger Stymphalia catchment ($\sim$ 182 km^2) and the smaller Kaisari catchment in the NE ($\sim$ 35 km^2) were connected in the early 20th century CE by an artificial tunnel (Knauss, 1990; Morfis and Zojer, 1986). Formerly, Lake Stymphalia drained via one main sinkhole (*katavothre*), which was encased in concrete in the 19th century (Morfis and Zojer, 1986). Today, water is pumped away for agricultural purposes via the Hadrianic aqueduct that was built around 130 CE and reactivated in the 19th century CE. Since the building of the aqueduct, lake level and size have varied considerably over time (Seguin et al., 2019).

Geologically, the Stymphalia Polje is located in the limestone and dolomite-dominated Gavrovo–Tripoli and Olonos–Pindos geotectonic zones, where karst features are abundant. Outcrops of the metamorphic phyllite–quartzite series, Neogene and Pleistocene conglomerates and marls, schists, and Quaternary deposits can be found mainly in the west and southwest (IGME, 1982, 1970; Morfis and Zojer, 1986).

The Kaisari Polje (37.93° N, 22.55° E, ca. 730 m a.s.l.) stretches ca. 7 km from the SW to NE directions. Morfis and Zojer (1986) considered it to be part of the Stymphalia Polje and called it valley of Klimenti, which is a village north of the village of Kesario/Kaisari (Fig. 1). It contained a small lake in former times, which was drained in the 1880s for agricultural purposes. The catchment geology of the Kaisari Polje is more homogeneous and consists of Neogene marls and conglomerates (Morfis and Zojer, 1986).

To the west of the Stymphalia Polje, crossing the Geronteion Pass in the Mavrovouni mountain ridge (rising up to 1600 m), the Pheneos Polje (37.85° N, 22.33° E) is located at approximately 700 m a.s.l. It is 28 km long and max. 13 km wide, with a catchment area of approximately 235 km^2 (Knauss, 1990; Morfis and Zojer, 1986). The ancient site of Archea Pheneos at the NW end of the polje (Fig. 1) was mainly inhabited during the Middle Helladic (ca. 4050–3650 BP).

Morfis and Zojer (1986) divide the Pheneos polje into an eastern and a western bay. It consists of two main hydrotectonic systems containing 87 springs and seven sinkholes (Morfis and Zojer, 1986). In this karstic environment, subsurface flow is of high importance for the hydrological system (Nanou and Zagana, 2018). Today, no perennial Lake Pheneos exists anymore and the water drains through trenches to the eastern *katavothre* (Fig. 2a). Most *katavothre* were anthropogenically regulated and the polje floor is no longer inundated, thus creating more space for agricultural land. Only during wet winter months may a small ephemeral/seasonal lake develop in the western bay (Morfis and Zojer, 1986). Today, the eastern *katavothre* is surrounded by a concrete construction to prevent it from blocking (Fig. 2c). Knauss (1990)

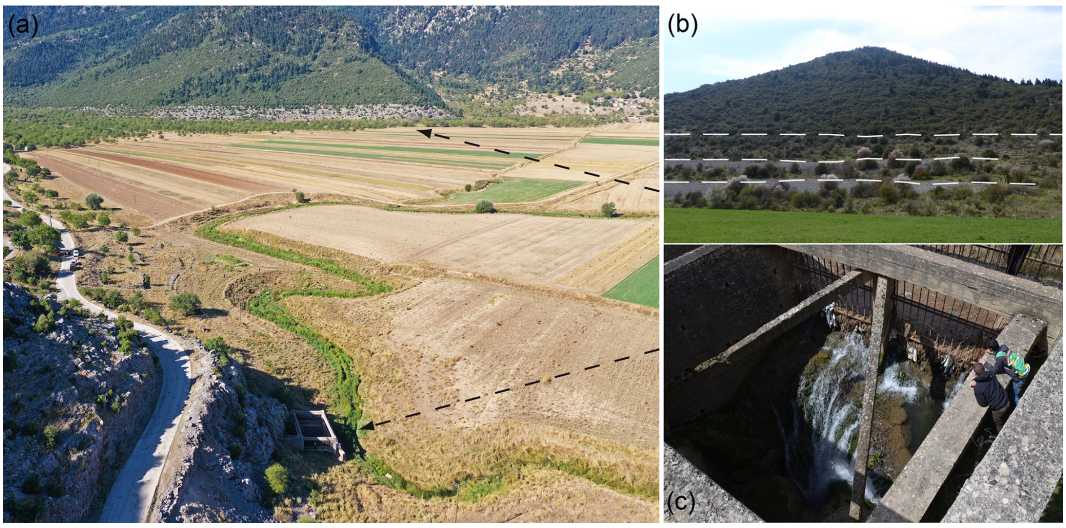

Figure 2. Photos of the Pheneos Polje. Locations are indicated in Fig. 1. **(a)** Aerial perspective with southwestward view on the eastern bay of the Pheneos Polje. **(b)** Side view on palaeoshorelines in the eastern bay close to Amigdalia. **(c)** Top-down view into the eastern *katavothre* contained in a concrete construction. The metal grille allows the discharge of water and prevents blockage. To the right, humans for scale (photos: Joana Seguin, 2017; Ingmar Unkel, 2019).

refers to different historical scholars who recount that it was blocked in the past more than once, causing inundations and high lake level stands, but they also report periods with complete desiccation of the polje. During the Ottoman period, the drainage system was purposely blocked in the 1820s, leading to a 39 km^2 large and 42.5 m deep lake, which was reopened by an earthquake in 1834 (Knauss, 1990).

Geologically, the Pheneos Poljes is similar to Stymphalia. It is likewise located in the limestone- and dolomite-dominated Gavrovo–Tripoli and Olonos–Pindos zones. Outcrops of the metamorphic phyllite-quartzite series, Neogene and Pleistocene conglomerates and marls, schists, and Quaternary deposits are also present (IGME, 1982, 1970; Morfis and Zojer, 1986).

The Asea valley is located in central Arcadia, close to Tripoli (Peloponnese) and about 50 km south-southwest of Stymphalia. Contrary to the geomorphologically closed poljes, the Asea valley, although located on the southwestern margin of the large Tripoli polje, is hydrographically connected to the catchments of the rivers Alpheios and Eurotas, both draining into the Ionian Sea, and thus Asea represents a natural thoroughfare (Unkel et al., 2014). Archaeological information for the site from Palaeolithic to early modern times is available from a field survey in the 1990s (Forsén and Forsén, 2003). Geologically, Asea belongs to the Gavrovo–Tripoli zone, characterized by carbonate rocks and some clastic flysch (IGME, 2002, 1992; Morfis and Zojer, 1986; Unkel et al., 2014).

3 Materials and methods

The methods applied equal the analyses of the sediment cores from Stymphalia (STY1) and Asea (Asea-1) (Heymann et al., 2013; Seguin et al., 2019; Unkel et al., 2014; Table 1), which allows detailed comparisons with our newly recovered records Pheneos (PHE1) and Kaisari (KES2).

3.1 Sediment coring

Fieldwork at the former lake sites of Kaisari and Pheneos was conducted in spring 2017. At the time of coring, both sites were drained and covered by pastures and non-vegetated field, thus being accessible for land-based vibracore drilling. Following a test coring using an open system (A cores), two parallel cores (B and C) for each site with a vertical offset of 50 cm were retrieved in 1 m sections of 55 mm diameter using inliner tubes deployed in a piston corer (Stitz type). PHE1 (37.85114° N, 22.33510° E; 390 cm total length) was cored in the eastern bay of the Pheneos Polje in proximity to the eastern *katavothre*. Two corings were taken from the Kaisari Polje, and we here present results from KES2 (37.94558° N, 22.57641° E; 350 cm total length), which is assumed to have been closer to the former lake depocentre. The sediment cores were kept in their sealed inline PVC tubes and transported to Kiel University (Germany), where they were stored at +4 °C in a cooler.

3.2 Sedimentology and geochemistry

After the cores from Pheneos and Kaisari had been split, they were described in terms of lithology, sediment texture, structure, and colour according to Munsell soil colour charts

Table 1. Overview of coring sites discussed in this study.

ID	Location	Core acronym	Coordinates	Elevation (m a.s.l.)	Catchment size	Presented core length
1	Stymphalia	STY1	37.84944° N, 22.46056° E	610	182 km^2	324 cm
2	Kaisari	KES2	37.94558° N, 22.57641° E	730	35 km^2	350 cm
3	Pheneos	PHE1	37.85114° N, 22.33510° E	710	235 km^2	390 cm
4	Asea	Asea-1	37.37603° N, 22.26592° E	630		500 cm

(Munsell, 2000). A master depth scale was established for each site based on a compilation of overlapping parallel cores using the RGB colour values. The core sections were visually correlated using distinct marker layers.

Fresh and smooth core surfaces of the archive half cores were prepared for line-scan photography (resolution: 143 ppcm cross-core and down-core, shutter time: 5 ms) and subsequently analysed geochemically via non-destructive X-ray fluorescence (XRF) scans using an Avaatech XRF core scanner (Richter et al., 2006) and an attached colour line-scan camera. The defined overlapping intervals in the parallel cores were scanned in two runs with 10 kV (exposure time of 10 s at 750 µA) and 30 kV (exposure time of 20 s at 2 mA, using a Pd thick filter) at a resolution of 5 mm. Combining the data into a continuous sequence and data cleaning were done in R version 3.5.1 (R Core Team, 2019). Cleaning of the dataset, i.e. the removal of explicit outliers and refilling of the missing values by linear interpolation, was done manually prior to statistical processing. Voids in the sediment, e.g. in PHE1 275–300 cm and in the topmost parts of both cores, were not filled with interpolated data. We selected 10 elements that were measured in all cores (10 kV: Al, Si, K, Ca, Ti, Mn, Fe; 30 kV: Rb, Sr, Zr) for detailed analyses along the sediment sequence. The XRF scanning results are expressed as element intensities that were transformed into centred log ratios (Weltje et al., 2015). Unlike element intensities, centred log ratios of elemental pairs minimize measurement variation caused by sample geometry, physical properties, and the closed-sum effect (Weltje and Tjallingii, 2008). Centred log ratio (clr) transformed data were also used for multivariate statistical operations.

Data exploration was conducted by statistical analyses using the open-source programme R (R version 3.4.2; R Core Team, 2019). For each study site, we applied a standardized and rotated principal component analysis (PCA) to the geochemical elements to reduce the dimensions that explain the variability in the dataset in the first place and secondly to explore the relationship between the different elements and their distribution within the sedimentary units. These principal components (PCs) do not have absolute units but reflect relative changes in the chemical composition over time. Element correlations of all elements acquired by XRF scanning were explored by biplots (Aitchison and Greenacre, 2002), which show the correlation of each element with respect to the main variance in the data indicated by principal components. For each lake ecosystem, the interpretation of element ratios as proxies for palaeoenvironmental variation needs to be explored and validated individually prior to multi-site comparisons (Xu et al., 2010).

For discrete samples from KES2 and PHE1, the grain size distribution < 2 mm was measured on air-dried samples (ca. 0.3 g, $n = 21$) every 30 cm using a laser particle analyser Malvern Mastersizer 2000. The samples were pretreated with hydrogen peroxide (H_2O_2, 35 %) to remove the organic matter, and the dispersant agent sodium pyrophosphate ($Na_4P_2O_7$) was added to avoid aggregation of particles. At least one measurement was conducted per previously identified lithological unit. The grain size distribution was categorized according to the DIN EN ISO 14688-1 nomenclature and indicated in volume percent (Figs. 4 and 5). However, grain size determination via laser diffraction on carbonate-rich sediments is known to be difficult (Murray, 2002), and thus it only provides general guidance here. In addition to laser diffraction, we use clr(Zr/Rb) as an indicator for variation in grain size of the clastic input (Figs. 4, 5), where lower values reflect finer-grained, clay-size particles (Dypvik and Harris, 2001).

Additionally, samples for carbon and nitrogen analyses were taken at the same intervals. The concentrations of total carbon (TC), total inorganic carbon (TIC), and total nitrogen (TN) were determined on dried and powdered samples using a Euro EA (elemental analyser). We calculated total organic carbon (TOC) concentrations in dry sediment by subtracting TIC from TC. The TOC/TN ratio was calculated to indicate the origin of the sedimentary organic matter. While values for autochthonous organic matter, such as algal biomass, are low, generally ranging between 4 and 10, land-plant organic matter eroded into the lake shows values higher than 10 and vascular plants even higher than 20 (Meyers, 2003).

3.3 Radiocarbon dating and Bayesian modelling

The radiocarbon dates used here from Stymphalia are published in Heymann et al. (2013) and Seguin et al. (2019) while those from Asea are published in Unkel et al. (2014). The chronologies of the new sediment cores from Pheneos and Kaisari (Table 2) are based on accelerator mass spectrometry radiocarbon (^{14}C) measurements performed at the Poznań Radiocarbon Laboratory.

Table 2. List of radiocarbon samples taken from PHE1 and KES2. The sampling depths refer to the master core. Indicated ^{14}C ages are unmodelled ages giving the 68.2 % calendar dating probability. Indicated IntCal13 ages are cal BP ages modelled with rcarbon using the IntCal13 calibration dataset (Reimer et al., 2013).

Sample no.	Core ID	Analysis no.	Sample material	Sample fraction	C content in this fraction[1] (mg C)	Conventional ^{14}C age $\pm 1\sigma$ (BP)	Calibrated ^{14}C age (cal BP), 1σ-ranges	Depth (cm)	Remarks
KES103 1465–1475 1510	KES-2c	Poz-95623	bulk sediment	alkali residue	> 1.0	1515 ± 30	1350–1414	103	
KES169	KES-2c	Poz-95624	bulk sediment	alkali residue	0.9	2775 ± 35	2799–2822 2843–2894 2901–2924	169	
KES240	KES-2c	Poz-95564	bulk sediment	alkali residue	0.4	3420 ± 35	3613–3706	240	
KES282	KES-2c	Poz-95625	bulk sediment	alkali residue	0.2	4530 ± 50	5059–5114 5117–5185 5215–5222 5238–5241 5266–5306	282	
KES332	KES-2c	Poz-95626	bulk sediment	alkali residue	> 1.0	2825 ± 30	2879–2914 2916–2958	332[2]	broken vial – contaminated
PHE075	PHE-1b	Poz-95627	bulk sediment	alkali residue	0.5	4080 ± 40	4450–4465 4518–4625 4764–4788	75[2]	
PHE095	PHE-1c	Poz-98167	bulk sediment	alkali residue	> 1.0	4890 ± 40	5595–5647	95[2]	
PHE128	PHE-1c	Poz-95628	bulk sediment	alkali residue	0.9	4850 ± 40	5489–5504 5582–5615 5628–5642	128[2]	
PHE149	PHE-1b	Poz-98169	bulk sediment	alkali residue	> 1.0	4825 ± 30	5486–5508 5581–5600	149[2]	
PHE186	PHE-1c	Poz-95630	bulk sediment	alkali residue	0.8	3180 ± 35	3376–3413 3421–3445	186	
PHE225	PHE-1b	Poz-95565	bulk sediment	alkali residue	> 1.0	4100 ± 30	4528–4626 4763–4789 4795	225	
PHE-256	PHE-1b	Poz-106235	bulk sediment	alkali residue	0.5	5870 ± 40	6656–6737	256	
PHE348	PHE-1b	Poz-95797	bulk sediment	alkali residue	0.2	8640 ± 60	9539–9634 9641–9660	348	

Notes: [1] Amount of remaining sample material after respective pretreatment. [2] Dates have been excluded from age–depth modelling.

For Pheneos and Kaisari, bulk sediment samples were taken for dating using the alkali residue fraction, due to the absence of discrete organic macro-remains during visual examination. Tephra layers supporting the chronology could not be found in the sediments and have so far not been reported in southern Greece for the Middle to Late Holocene in this area (Zanchetta et al., 2011). Poor preservation of organic matter and the high amount of reworked material and inorganic carbon content present a considerable challenge for precise ^{14}C dating in the semi-arid Mediterranean (Grootes et al., 2004; Vaezi et al., 2019; Walsh et al., 2019). As human decisions may have a strong influence on the age–depth modelling, we present our dating proceeding in detail in the following.

The age–depth models of Pheneos and Kaisari were produced using rbacon (Blaauw and Christeny, 2011) with respect to the IntCal13 calibration curve (Reimer et al., 2013) and without applying any reservoir correction (Fig. 5).

For the Pheneos sequence, we calculated the age–depth model PHE_03 based on eight samples (Table 2) for the complete master core of 390 cm (Fig. 5). The analysis of the sediment sequence gave no indications for hiatuses or erosional discontinuities, and thus a continuous sedimentation was assumed. The lithology of the upper half of the core however seems different and most probably reflects higher input of terrestrial material. Four samples taken from units 7 and 8 (PHE075 – PHE149) all show an age reversal of up to 3000 years, indicating contamination by old detrital car-

bon (Seguin et al., 2019) and were hence excluded from the modelling process.

For the Kaisari sequence, four bulk samples were used (Table 2) along the 350 cm core (Fig. 5). The top of the sediment cores in Kaisari and Pheneos was disturbed by agricultural activity, and the uppermost sedimentological unit was considered to be plough horizon at both sites. Hence, it was not used for dating, and the date of the surface was defined as the year of coring (-67 ± 10 BP).

For Asea, charcoal and plant remains from 30 sediment intervals were handpicked, pretreated, and radiocarbon dated by NOSAMS at Woods Hole Oceanographic Institution (see Table 1 in Unkel et al., 2014). The initial age–depth model was published in Unkel et al. (2014); it was calculated using Oxcal 4.1 and based on IntCal09 (Reimer et al., 2009). Based on the most recent state of knowledge and for the sake of consistency in the inter-comparison, the model was also updated here using rbacon and IntCal13 as a calibration curve (Reimer et al., 2013, Fig. S1). As sample nos. 229 and 236, i.e. charcoal material, most likely gave too old of ages, we considered them here as outliers. Sample nos. D, L, M, N, 233, and 235 were considered too young of ages, as they contained root fragments probably penetrating the sediment post hoc, e.g. reaching to the aquitard (greenish grey units 2–3)" (Unkel et al., 2014). They were likewise considered to be outliers and excluded from modelling (Fig. S1).

For Stymphalia, the data and modelling approach is described in detail in Seguin et al. (2019). It is based on 45 radiocarbon measurements on 26 samples, modelled with rbacon and calibrated using IntCal13 as the calibration curve (Reimer et al., 2013). For bulk sediment samples, we regarded the humic acid fraction as providing more plausible results than the alkali residue fraction, and we applied a reservoir correction of 200 ± 100 years. Cultural dates such as the building of the Hadrianic aqueduct and the finding of a ceramic sherd were additionally integrated into the modelling approach.

If not stated otherwise, mean ages were extracted for all models and used for representation and interpretation of the geochemical proxies. In the following, all dates are indicated as calibrated calendar years before present (cal BP), where "present" is defined as 1950 CE with 1σ-uncertainty ranges according to Mook and van der Plicht (1999).

4 Results

4.1 Lithostratigraphy and geochemistry

The lithology of the Stymphalia core STY1 is presented by Heymann et al. (2013) and Seguin et al. (2019). The upper 324 cm was distinguished into 20 lithological units (units 54–70b). The colours are generally brighter in the upper half; a distinct blackish layer (unit 62) separates the upper brownish units from the lower, darker greyish units (Seguin et al., 2019).

Similar to the other sites, the sequence presents fine sediments dominated by silt. Contrary to the other cores, shell fragments of *Bithynia* sp. and *Valvata* sp. gastropods appear frequently.

For the Asea core, 11 lithological units were differentiated, and the sequence has a fine texture of clay to silt size particles with few intercalations of smaller carbonate clasts and isolated pebbles. The colours range from very dark greyish brown at the bottom to dark olive brown at the top, generally becoming brighter towards the top except for the blackish unit 9 (Unkel et al., 2014).

4.1.1 Pheneos

Core PHE1 stretches over 390 cm and nine lithological units (Fig. 3, Table S1). The upper 19 cm is missing due to unconsolidated material and core compaction. Due to an unfortunate match of coring depths of parallel lower core segments, a void exists at 276–290 cm.

Colours range from 10YR 3/1 to 10YR 5/3 (Munsell, 2000) with brown and dark yellowish brown colours characterizing the sediments. The lower part of the core is generally darker than the upper half, except for the bright unit 1 (Fig. 3). The transitions between the units are all gradual and do not show signs of abrupt changes. Visible organic debris is absent except for some modern roots in the plough horizon (unit 9). Very few mollusc shell fragments were found in units 6 to 8. The TOC content varies between 0.2 wt %, at the boundary between units 1 and 2, and 2.3 wt % in the uppermost unit (Fig. 3). The existence of numerous carbonate concretions within the rather fine matrix of the sediment in several intervals of the core is characteristic and points towards at least seasonal desiccation and initiation of soil formation. A higher number of carbonate concretions with diameters < 0.5 cm occurs in units 1 and 4. TIC (ranging from 0.6 to 4.0 wt %) and Ca contents follow a similar trend, showing the highest values in unit 1 and low values in units 2 and 5. Total nitrogen (TN) ranges from 0.04 to 0.16 wt % with an average of 0.08 wt %. The TOC/TN ratio ranges from 4.8 to 21.6, indicating varied mixing of aquatic algae and terrestrial vascular plant material (Meyers, 2003). Units 2 and 4 show the lowest TOC/TN ratios, suggesting a greater input of autochthonous aquatic algae.

The grain size distribution ranges from fine to medium silt; it has a mean clay content of 20.4 vol %, a mean silt content of 78.1 vol %, and a mean sand content of only 1.5 vol %. The uppermost unit 9 is of homogeneous brown colour and has an exceptionally high clay content > 30 vol %, which may be linked to alteration and compression by agricultural use of the area. Due to this modern anthropogenic alteration, unit 9 is excluded from any palaeoenvironmental interpretation.

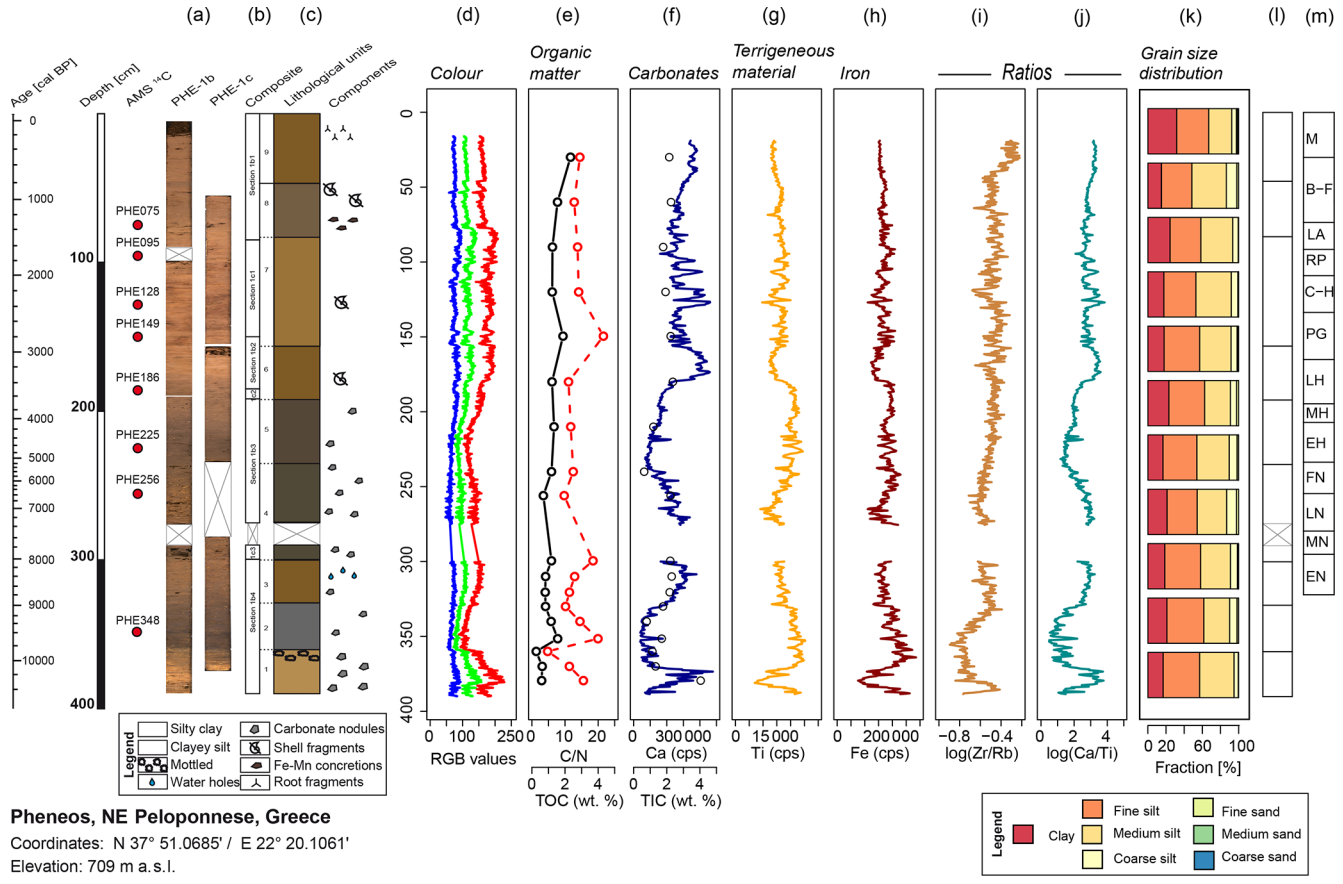

Figure 3. PHE1 composite core log with pictures **(a)**, master core profile **(b)**, lithological units **(c)**, and overview of different proxies plotted against depth. Age scale is adapted to depth scale. Depths where samples for ^{14}C dating were taken are marked by red dots. **(d)** RGB colour values (blue, green, red). **(e)** TOC (black line) and TOC/TN (red dotted line). **(f)** TIC (circles) together with counts per second (cps) of calcium (dark blue line). **(g)** Titanium (in cps). **(h)** Iron (in cps). **(i)** Log ratio of Zr/Rb. **(j)** Log ratio of Ca/Ti. **(k)** Granulometry. For orientation, boxes with lithological units **(l)** and cultural periods **(m)** are indicated (for abbreviations and temporal classification of cultural periods see Table S3 and Weiberg et al., 2016).

4.1.2 Kaisari

The core KES2 has a length of 350 cm, while the upper 34 cm of unconsolidated material is missing. Most analyses including XRF scanning exclude the upper 50 cm, as the material was too loose to meet the scanning prerequisites. KES2 was subdivided into seven lithological units (Fig. 4, Table S2). No laminations are visible, all unit boundaries are gradual and do not show any sign of abrupt changes, hiatuses, or event layers. Overall, the core looks very homogeneous; yellowish brown to olive-brown colours (10YR 4/4 to 2.5Y 5/3; Munsell, 2000) are dominant. Reddish mottled sections with a higher Fe content suggest that the coring spot periodically dried out and oxidation processes occurred. However, fractures, layers of gypsum, or carbonate nodules, which could indicate desiccation or soil formation, are absent. With the beginning of unit 6, few patches of reddish material appear, which suggests the selective input of reddish soils present in the catchment. Macro-remains are likewise largely absent except for some roots in the plough horizon (unit 7) and sporadic, small shell fragments in the lower part of the core. Intact gastropod shells – abundant in Lake Stymphalia – are absent here. The sediment sequence has a fine, silty texture composed of a varying mixture of clay (mean = 21.5 vol %) and silt (mean = 77.5 vol %); sand content was < 1 vol %. TOC varies between 1.0 wt % and 2.2 wt %. TN is similar to Pheneos and ranges from 0.06 wt % to 0.13 wt % with an average of 0.09 wt %. TOC/TN ratios are in the range of 14–27, which – in contrast to Pheneos – indicates a predominantly or exclusively terrestrial source of organic matter with a higher input of vascular plants (TOC/TN > 20) in units 2 to 4.

4.2 Core chronologies and sedimentation rates

The 390 cm long Pheneos core covers a total time span of 10 500 years (Fig. 5a). On average, the sedimentation rate for the whole sequence was calculated at approximately 0.37 mm yr^{-1}, being lowest between 4500 and 6500 cal BP

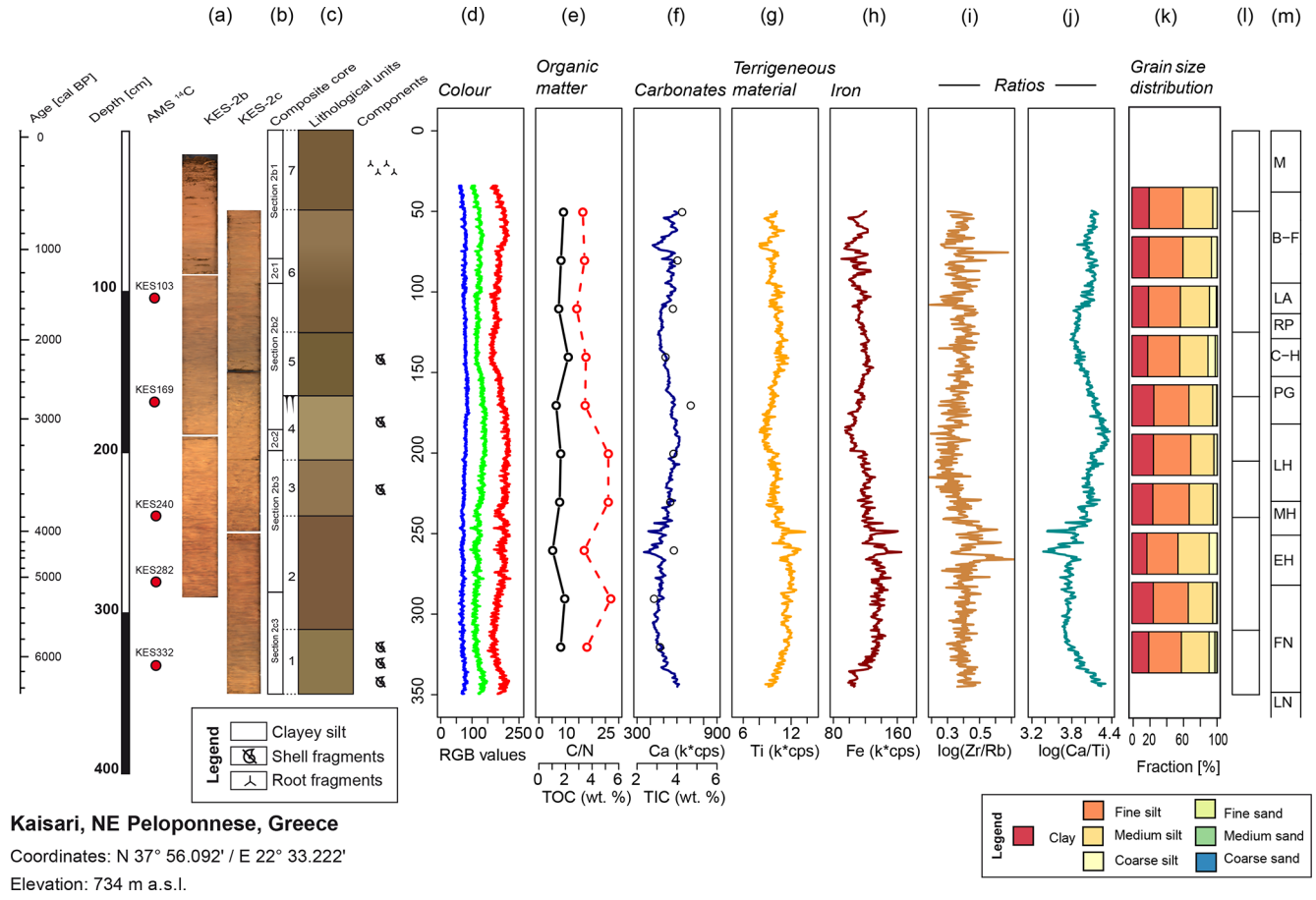

Figure 4. KES2 composite core log with pictures **(a)**, master core profile **(b)**, lithological units **(c)**, and overview of different proxies plotted against depth. Age scale is adapted to depth scale. Depths where samples for ^{14}C dating were taken are marked by red dots. **(d)** RGB colour values (blue, green, red). **(e)** TOC (black line) and TOC/TN (red dotted line). **(f)** TIC (circles) together with calcium (dark blue line, in 1000 × cps). **(g)** Titanium (in 1000 × cps). **(h)** Iron (in 1000 × cps). **(i)** Log ratio of Zr/Rb. **(j)** Log ratio of Ca/Ti. **(k)** Granulometry. For orientation, boxes with lithological units **(l)** and cultural periods **(m)** are plotted to the right (for abbreviations and temporal classification of cultural periods see Table S3 and Weiberg et al., 2016).

with ca. 0.16 mm yr^{-1}, slightly increasing to 0.32 mm yr^{-1} between ca. 4800 and 3300 cal BP, and further increasing to ca. 0.53 mm yr^{-1} during the last 3000 years.

Based on the age–depth model KES2_01 (Fig. 5b), we calculated the average sedimentation rate to be approx. 0.54 mm yr^{-1} with a slightly higher accumulation rate (0.78 mm yr^{-1}) between 3800 and 2800 cal BP.

For Asea, the initial age–depth model by Unkel et al. (2014) was updated by a more sophisticated modelling approach. Now, the 500 cm long core covers a time span of 5400 years. Our new age–depth model shifted towards younger ages by up to 1000 years compared to the Unkel-2014 model, especially during the third millennium cal BP (Fig. S1). According to the new age–depth model (Asea_9), the average sedimentation rate for Asea is calculated to 0.92 mm yr^{-1}. For the period 3000–3600 cal BP, the rate is considerably lower with approximately 0.3 mm yr^{-1}.

So far, the upper 5 m of the Stymphalia STY-1 core has been studied geochemically in high resolution (Seguin et al., 2019; Heymann et al., 2013). The most recent age–depth model was calculated for the upper 324 cm, indicating a basal age of 8500 cal BP (Seguin et al., 2019). This gives an average sedimentation rate of 0.38 mm yr^{-1} for the total sequence. For the period 8500–2000 cal BP, the rate is calculated to be approximately 0.2 mm yr^{-1}. It rises to 0.4 mm yr^{-1} around 195 cm and strongly increases to more than 2 mm yr^{-1} at 165 cm. For the uppermost 50 cm, a lowering of the sedimentation rate to 0.7 mm yr^{-1} was calculated (Seguin et al., 2019).

Asea-1 shows a consistently higher average sedimentation rate than the other three sites (Fig. 7). For 6500–3500 cal BP, the sedimentation rate in STY1 and PHE1 is similar and increases in younger times. For KES2, the sedimentation rate stays relatively constant over the whole period, which can

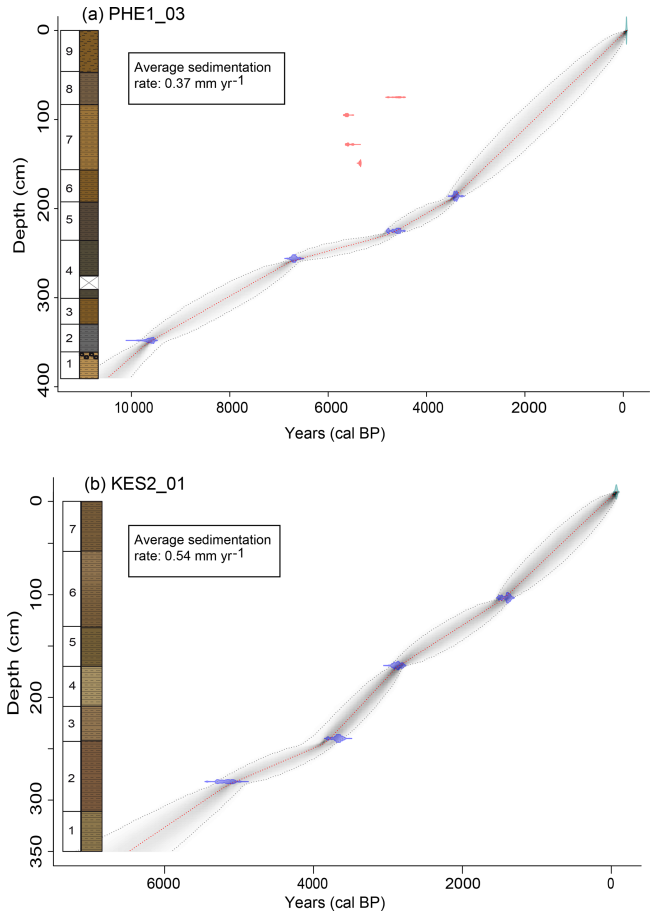

Figure 5. Bayesian age–depth models for Pheneos **(a)**. Kaisari **(b)**. The models were constructed using the R package *rbacon* (Blaauw and Christeny, 2011). The blue tie bars indicate the ^{14}C age distributions (see Table 2). Outliers are plotted in red and were excluded from modelling (explanation in the text). The greyscale of the line graph reflects the likelihood: the darker the more likely the model passes through that age. The red dotted line follows the mean ages. The core lithologies are plotted to the left.

mainly be attributed to the lowest available number of radiocarbon dates.

In the following, we compare and interpret all four archives palaeoenvironmentally for the last 5000 years, since the beginning of the Helladic period (Table S3), a period when the Greek societies were sedentary and generally achieved major advances in social, economic, and technological skills (Bintliff, 2012).

4.3 Statistical analyses of the geochemical data

The principal component analysis, based on clr-transformed data, revealed comparatively similar patterns for all for sites (Fig. 6). The first two principal components (PC1 and PC2) for each site account for $>65\,\%$ of the variance in the respective dataset. For Stymphalia, PC1 explains 62.5 % of the variance and is negatively associated with Ca and Sr and positively associated with elements in clastic materials. For Kaisari and Asea, the relationship is similar and PC1 explains 43 % and 46.1 % respectively (Fig. 6). For Pheneos, PC1 also spans the axis between carbonate and terrigenous assemblages (53.1 %), but Sr appears more distant from Ca and closer to Si, indicating an additional non-carbonaceous Sr source, e.g. feldspars (Kylander et al., 2011). Generally, the loadings of Ca and Sr in carbonates are closely bound together and point to one axis direction, while the loadings of elements such as Al, Fe, K, Rb, Si, Ti, and Zr in clastic material show a wider spread of directions, but largely point to the opposite direction of the carbonates, indicating a high negative correlation (Fig. 6). The influence of K is the most variable in the four archives and more strongly influences PC2. Mn plots perpendicular to most of the other elements, indicating that it is influenced by an independent process.

A colouration of the point cloud by depth (Fig. 6) visualizes the geochemical evolution of the lake ecosystem and intervals where general geochemical changes become visible or abrupt changes are revealed. For Asea, for example, the upper lithological unit has not been interpreted palaeoenvironmentally, because post-depositional processes have caused the precipitation of carbonate nodules (Unkel et al., 2014). This can be observed in an abrupt shift in the biplot towards very Sr- and Ca-rich samples (Fig. 6).

For a comparison of all sites, the clr(Ca/Ti) ratio, showing higher correlations for all sites, seemed to be more suitable to depict this relationship than clr(Rb/Sr), which was applied as a palaeoenvironmental proxy for Stymphalia (Seguin et al., 2019). It was thus compared to PC1 and plotted over time (Fig. S3) to demonstrate similarities and to illustrate the highest fluctuations of geochemical proxies in the respective dataset.

5 Discussion

5.1 Archive comparison on the spatial scale

Our analyses of the four sediment cores revealed considerable variation within the proxies, which shows that the landscape in NE Peloponnese has changed significantly over the last 5000 years. Changes in the proxies can be interpreted on different spatial and temporal scales. Microscale changes occur due to local forcing that only influences one lake catchment and hence is not visible in the neighbouring poljes. They may also hint towards anthropogenic activities in the respective valley. Archaeological evidence at the study sites, however, is limited to specific periods. Human activity within the lake catchments certainly had an impact on erosion processes and water availability (Seguin et al., 2019), but archaeological information is often lacking and it is not always evident to differentiate clearly anthropogenic and natural drivers in the geochemical record of the sediment. On a mesoscale, we find regional, climatic similarities across the Peloponn-

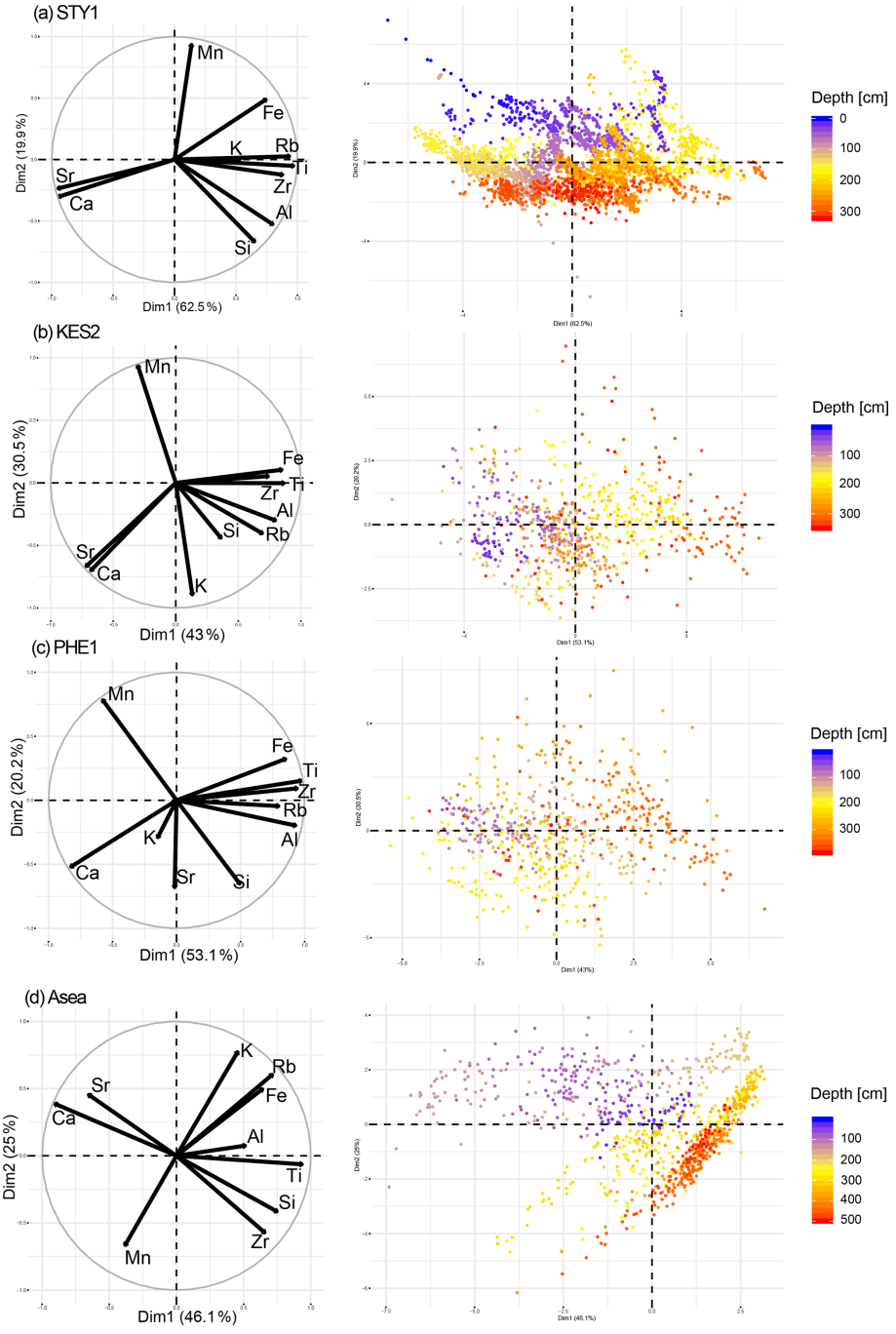

Figure 6. Principal component analyses (PCA) for all study sites. (left) Variable correlation circles of PCA of the XRF data for each site displaying correlation between PC1 (Dim1) on the *x* axis and PC2 (Dim2) on the *y* axis. (right) Distribution of sample points in the PC1–PC2 scatter plot for each site. The samples are coloured according to their depth in the sediment core from purple (surface) to red (maximum depth). The point density for STY1 is highest because data resolution is 1 mm. For the interpretation, the reader is referred to the text.

nese visible in all four sites, while macroscale changes can be linked to over-regional climatic phenomena also visible in further proxy records from Greece and adjacent regions.

All study sites represent shallow lacustrine environments that were not permanently waterlogged during the respective period, but rather show phases of periodic or episodic desiccation. Although Pheneos, Stymphalia, and Kaisari are located in the immediate proximity (Fig. 1) and may have experienced the same climatic changes, the sedimentary facies vary significantly due to differences in catchment size, lake size and depth, and geology. Common features of all sites are a relatively low organic carbon content and the very low

abundance of sand-sized particles within the grain size distribution. Fine-grained silty clay and clayey silt dominate the Pheneos and Kaisari sequences. Sand and coarse matrix (> 2 mm) are almost absent with the exception of carbonate nodules in PHE1 (Fig. 4). No event layers were identified, and boundaries between the sedimentary units are exclusively gradual in Pheneos and Kaisari. Combined with the dominance of fine material, this indicates rather constant deposition of sediment under relatively stable or gradually changing conditions and excludes the existence of slumped units deposited during extreme precipitation events or earthquakes. Accordingly, the sediment sequence in Kaisari only shows very slight variations in the geochemical proxies (Fig. 4). The catchment and the transport distance from the slopes to the coring spot are much smaller, and the input of terrestrial detritus is thus higher compared to Pheneos or Stymphalia. Comparatively stable counts of terrigenous elements suggest that the input of clastic detritus was relatively constant during the Middle and Late Holocene, which is likewise supported by the rather stable sedimentation rate.

A comparison of all four age–depth models (Fig. 7) shows a generally higher resemblance for the age–depth curves for the three poljes surrounding Mt. Ziria, while the model for Asea shows a significantly higher sedimentation rate. While Stymphalia and Pheneos have similar sedimentation rates in the lower part (> 3800 cal BP), Kaisari shows an overall more constant and slightly higher deposition rate, which can be ascribed to the softer and more easily erodible marl sediments in the catchment and the smaller lake size, where allochthonous detrital material from the slopes reaches the coring site more easily. In Stymphalia, a strong increase in the sedimentation rate related to anthropogenic activity was observed around 1200 cal BP (Seguin et al., 2019). In Pheneos, age constraints for the upper 185 cm are unfortunately weak, and we link the age reversals in unit 7 to higher input of old, terrestrial carbon, which may have been caused by increased erosion caused by human activity. Contrary to Stymphalia, we did not apply a reservoir correction to the chronologies for Pheneos and Kaisari, because this varies site specifically and may even change over time (Grimm et al., 2009; Stein et al., 2004). Due to the old carbon effect, it is more likely that the age–depth models for Kaisari and Pheneos indicate too old ages than the opposite (Grootes et al., 2004; Olsson, 1991). To account for discrepancies in the chronologies (see also Fig. S2), we restrict the analysis of variation in the dataset to the centennial scale and do not trace direct links between palaeoenvironmental and societal changes.

The 390 cm long Pheneos sediment sequence covers the last 10 500 years, while the bottom of the 350 cm long Kaisari core (KES2) was dated to 6500 cal BP. Both lakes have experienced at least periodic desiccation during the last 5000 years, which is indicated by the absence of visible organic macro remains, the low TOC content, and the carbonate nodules in Pheneos and the strongly mottled nature of the sediment in Kaisari suggesting turbation. Due to the non-stratified lithology with oxidized patches, low preservation of organic remains, and the absence of indications for anoxic conditions, the sediments of both palaeolakes suggest relatively shallow water levels and high water level fluctuations with a well-mixed and ventilated water column.

For all our study sites, the first principal component (PC1) explains the variation between carbonate-rich and mineral-rich assemblages (Fig. 6). Similar elemental distributions in PC1 have been found in Greece (Katrantsiotis et al., 2018) and in Tibet (Ramisch et al., 2018). We interpret these fluctuations as hydro-climatic variations. Intensified carbonate precipitation (low values of PC1) occurs during warm and dry summers, while the input of clastic material (high values of PC1) may be enhanced during wetter periods (Croudace and Rothwell, 2015; Heymann et al., 2013; Katrantsiotis et al., 2018). We use PC1 as the main palaeoenvironmental proxy in the following, as it represents all carbonate and siliciclastic elements by their loadings and thus is more representative than a ratio, based on only two elements, although the clr(Ca/Ti) reflects the same bipolar distribution between carbonate precipitation and terrigenous input and depicts similar trends (Fig. S3).

5.2 Palaeoenvironmental reconstruction on the temporal scale

Changes in water level and water availability may be attributed to climatic fluctuations as well as to human interference. The intensity and spatial distribution of human activities however is highly variable over time. There is much evidence that human activity in the Peloponnese increased with the introduction of Helladic economies (Weiberg et al., 2016). While low activities are assumed for most of the Final Neolithic (archeologically constrained for the period 6450–5150 BP), a population boom is inferred for ca. 4750 BP followed by another decline around 4350 BP (Weiberg et al., 2019). No explicit information is available on human impact in the studied valleys for the Early Helladic period. The onset of the Early Helladic period and thus the Greek Bronze Age in southern Greece is archaeologically defined at 5050 BP (Weiberg et al., 2016), and it can generally be assumed that human activity in the study area existed throughout the entire analysed period with varying intensities. According to Sadori et al. (2011), vegetation changes before ca. 4000 cal BP can be linked to climatic rather than anthropogenic forcing, which was locally restricted. The possible impacts of climatic changes on sedentary communities are a key topic in palaeoclimatic research in the eastern Mediterranean; they may have been one factor contributing to the downturn of societies, as intensely discussed for the Late Helladic Mycenaean palatial period (Drake, 2012; Finné et al., 2017; Kaniewski et al., 2013; Knapp and Manning, 2016; Knitter et al., 2019; for cultural phases see Table S3).

In the following, we present our data chronologically divided into three different periods; the limits were set accord-

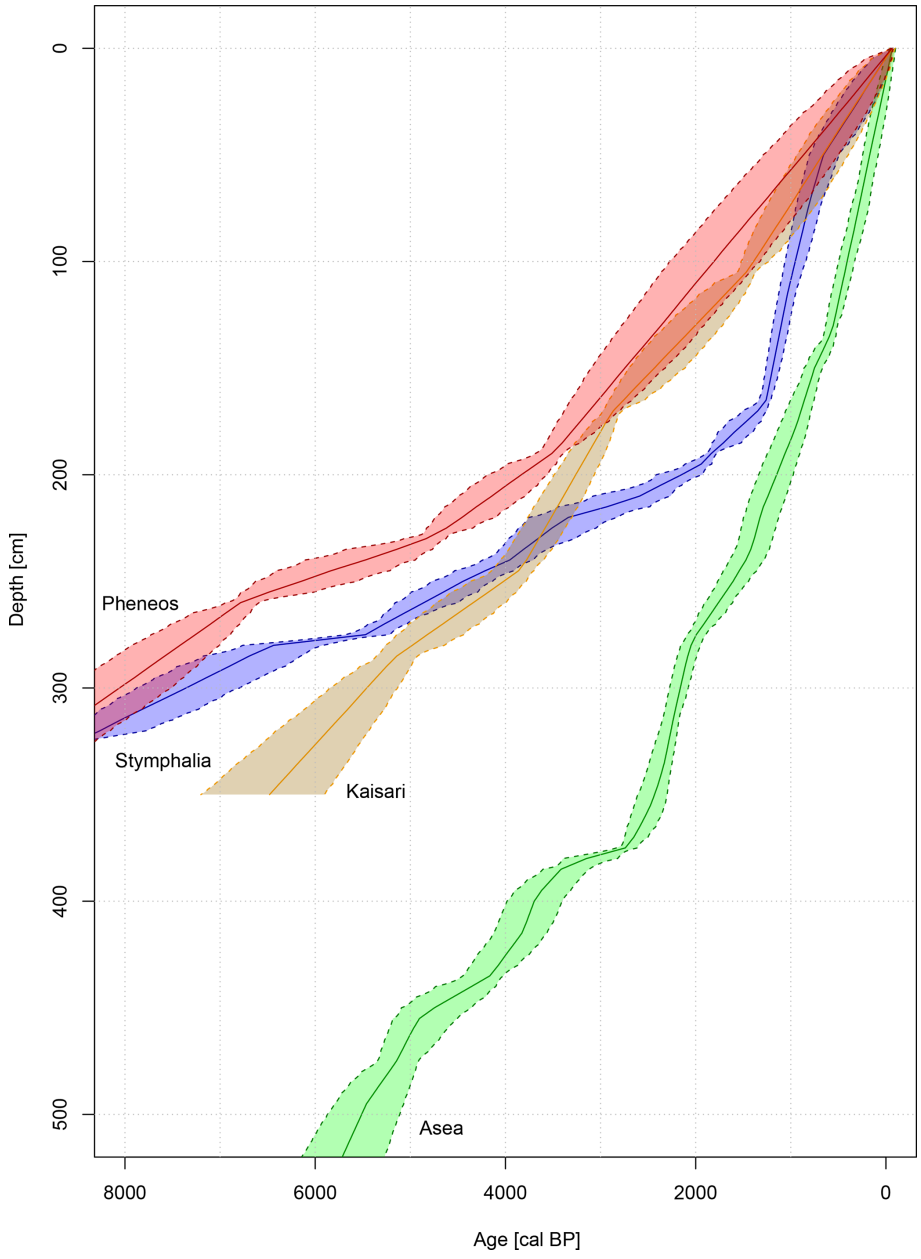

Figure 7. Comparison of age–depth models for all four study sites. Solid lines indicate the mean age of the respective model, while the dotted lines indicate the $\pm 2\sigma$ probability range. The shaded area reflects the possible age–depth distribution range.

ing to the boundaries of cultural periods of southern Greece as defined by Weiberg et al. (2016), to underpin the significance of human–environment interaction in the study area.

5.2.1 Early to Middle Helladic (5050–3650 cal BP)

For the Early to Middle Helladic period, our geochemical proxies generally indicate wetter conditions. In Pheneos, phases of blackish sediment colour with higher Fe content and slightly higher TOC content hint towards less oxygenated phases, in which the non-composed organic matter and reduced iron minerals, e.g. iron sulfides, most probably cause the blackish colouration. In combination with low Ca content, this generally indicates phases of lower evaporation and more permanent water saturation around 5100–3600 cal BP (unit 5; Fig. 4). This is further supported by TOC/TN ratios of ± 12, which indicate a mix of terrestrial and aquatic organic matter (Meyers and Ishiwatari, 1993). It thus seems as if during this period, wetter conditions prevailed and the eastern Pheneos Bay was covered by a permanent lake. In Kaisari, the geochemical proxies and the lower TOC/TN ratio at 260 cm also indicate wetter conditions at

the same time, but generally a higher variability. Asea shows very stable conditions over the period 5000 to 3400 cal BP with two short, dry pulses around 4900 and 4700 cal BP and a general tendency towards increasingly wetter conditions. The PC1 in Stymphalia likewise depicts wetter conditions approximately until 4200 cal BP, when it reaches stable mean values for the following 250 years. This is in agreement with a humid period reported from Agios Floros (Fig. 8g; Norström et al., 2018) as well as with results from a marine sediment core from the NE Aegean Sea (Triantaphyllou et al., 2016) indicating continuous warm and humid conditions between 5.5 and 4.0 kyr BP terminating with the "4.2 kyr" climate event.

The 4.2 kyr event is often described as a period of increased aridity and drought conditions in large parts of the Mediterranean (Finné et al., 2011; Isola et al., 2019; Kaniewski et al., 2018) and has recently been set as a time marker for the onset of the Late Holocene (Walker et al., 2019). In the Asea record, the event is completely absent (Unkel et al., 2014) and not clearly visible in our other three records either (Fig. 8a–d). In Stymphalia, PC1 may indicate a slight tendency towards drier conditions, while Pheneos and Kaisari show more prominent short-term fluctuations on a microscale level, representing higher fluctuations in the respective lake levels.

5.2.2 Late Helladic to Archaic (3650–2429 cal BP)

The Middle Helladic to mid-Late Helladic cultural period (ca. 4050–3300 cal BP) appears as a relatively stable phase at all four sites, which is supported by reconstructions from Lake Lerna (Katrantsiotis et al., 2019) and Agios Floros (Norström et al., 2018), although they have a much lower resolution. Following this more stable phase, several Peloponnesian records provide evidence for an aridification trend starting around 3300 cal BP. Changes in the geochemical proxies occur gradually; the most significant shift occurs in Pheneos and Kaisari around 3300–3200 cal BP. The input of terrigenous elements (e.g. Ti, Zr, K) decreases, while carbonate content increases (Figs. 4, 5). Although elements in siliciclastic material decrease in concentration, the accumulation rate indicates an increase which may derive from more intensified carbonate precipitation during drier conditions. This is supported by the bright yellowish brown colour of the sequences and reddish oxidized patches in the sediment, suggesting episodic desiccation. Climatologically, this can be interpreted as warmer summers leading to more evaporation and carbonate precipitation and lower input of allochthonous sediment due to less intense precipitation. While Pheneos and Kaisari depict rather continuous shifts that peak in 3000 cal BP, Asea and Stymphalia show two minor dry spells around 3200 and 2900 cal BP while the conditions in between seem wetter (Fig. 8a–d). This pattern looks similar to the records from Gialova and Lerna (Fig. 8e, f; Katrantsiotis et al., 2018; Norström et al., 2018). The differences in the reaction may be explained by age uncertainties, a diverging resilience in the respective ecosystems, or differing sedimentation processes. The considerable drying trend observed in Pheneos and Kaisari is generally in line with the Agios Floros record, Mavri Trypa, and Closani Cave, Romania (Fig. 8g, h, j; Finné et al., 2017; Katrantsiotis et al., 2015; Warken et al., 2018). Nevertheless, as the radiocarbon dates in Pheneos show age reversals for this period, it cannot be excluded that the material here has been reworked by relocation and transport and that the geochemical proxies do not depict a climatic signal for the respective time period.

The rapid climate change interval, as defined by Mayewski et al. (2004) for 3500–2500 cal BP, is characterized by pronounced but heterogeneous climatic shifts in many regions across the Mediterranean and Europe. Scaling up to the meso-level, some authors see a significant climate event at 3200 cal BP (3.2 kyr event) and relate it to cultural changes at the end of the Late Helladic period (Table S3), also understood as the end of the Greek Bronze Age (Drake, 2012; Finné et al., 2017; Kaniewski et al., 2013; Weiberg et al., 2016). Other studies find more evidence of a climatic shift around 2800 cal BP (2.8 kyr event; Neugebauer et al., 2015; van Geel et al., 2014), temporally related to the onset of the Greek Early Iron Age. The temporal and spatial diversity in the results of various studies shows that climatic changes proclaimed on a macroscale could be regionally very different and reveal very heterogeneous (local) conditions. This seems to be particularly the case during this time interval, while studies for other Holocene climate events, such as the 8.2 kyr or the 4.2 kyr events, reveal more homogeneous manifestations on the different scales (Bini et al., 2019; Isola et al., 2019; Zanchetta et al., 2016).

Several proxies confirm a drying trend in Greece at the end of the Late Helladic period (Emmanouilidis et al., 2018; Finné et al., 2017; Katrantsiotis et al., 2018, 2019; Warken et al., 2018). While other studies indicate an overall drying trend for ca. 3000–2000 cal BP, with a short break of one wetter phase or two separate dry phases, as observed for example at Agios Floros or Thassos Cave, Skala Marion, NE Greek island (Norström et al., 2018; Psomiadis et al., 2018). The juxtaposition of climate records shows that the end of the Late Helladic period was a period of high climatic instability, during which the majority of the records for southern Greece indicate a shift towards generally drier conditions, but with high intra-regional variability (Finné et al., 2011). We reason that based on the heterogeneous data, even on a mesoscale, one needs to examine studies critically that draw a direct causal link between climate fluctuations and cultural decline. In the records presented here, we mostly see gradual changes in the environmental proxies for the last 5000 years and suggest that climatic fluctuations in the NE Peloponnese have not been as rapid or drastic to cause a societal downturn. However, this may also partly be an effect of how the climatic signal is stored in the sediment; as these lakes did not produce varves or laminated sediments, we need to con-

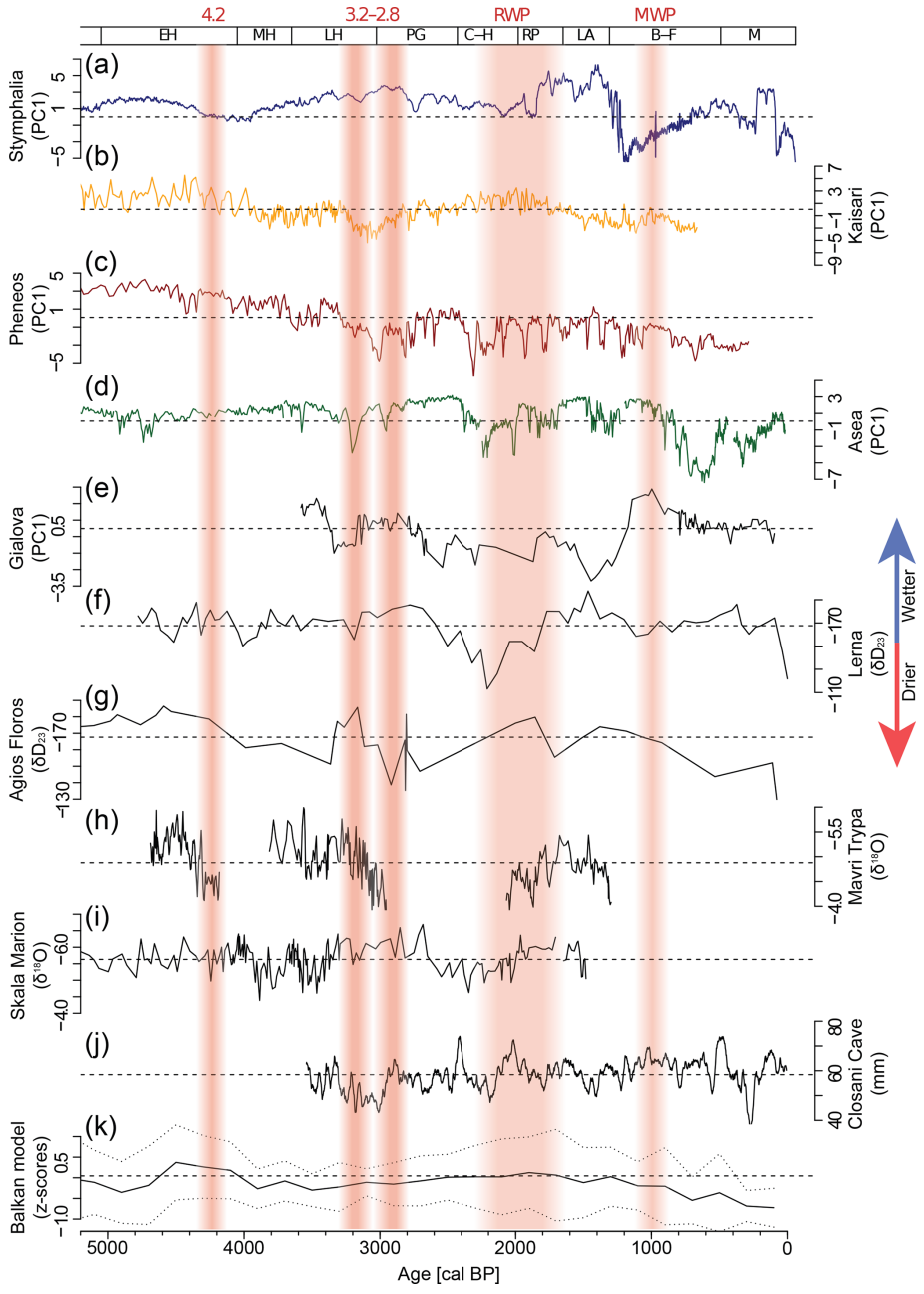

Figure 8. Comparison of the PC1 proxies (**a–d**, this study) with other regional records for the last 5000 years. **(e)** Gialova PC1 (Katrantsiotis et al., 2018). **(f)** Lerna δD_{23} (reversed; Norström et al., 2018). **(g)** Agios Floros δD_{23} (reversed; Norström et al., 2018). **(h)** Mavri Trypa $\delta^{18}O$ (reversed; Finné et al., 2017). **(i)** Thassos Cave $\delta^{18}O$, Skala Marion (reversed, Psomiadis et al., 2018). **(j)** Closani Cave, Romania, autumn–winter precipitation (Warken et al., 2018). **(k)** Regional mean and uncertainty range of the Balkan model based on 10, notably sedimentary, archives from the Balkan region (Finné et al., 2019). Horizontal dotted lines depict the respective mean values for each dataset. Vertical reddish shaded bars indicate periods with potentially drier or warmer climatic conditions (RWP: Roman Warm Period; MWP: Medieval Warm Period).

sider the possibility that proxy signals have been smoothed out over a few years. Nevertheless, as we detect no severe climatic events in any of our records, we assume that climatic changes may have been only one factor in a multi-causal relationship influencing cultural transformations.

Human-induced vegetation clearing also increases erosion and may cause similar signals in the sediment like an increase in precipitation and surface run-off. Thus, the shifts observed in Pheneos and Kaisari around 3300–3200 cal BP could likewise be explained by anthropogenic forcing. Late Helladic

activity is attested for the Stymphalia Polje only by some pottery sherds (Williams, 2013). In the Kaisari Polje, Late Helladic settlement activity is attested by pottery at the northern fringe of the plain, and later there is some evidence of human activity in Archaic and Classical times (Lolos, 2011). For Asea, we know about human activity due to an archaeological survey (Forsén and Forsén, 2003), but we do not have any clear evidence from excavations to distinguish human and climate influences in the record (Unkel et al., 2014). In the Pheneos Polje, pottery from the Late Helladic period to Early Iron Age (ca. 3150–2650 BP) was found in archaeological surveys, but without clear stratigraphical information (Erath, 1999; Howell, 1970; Tausend, 1999). According to Knauss (1990), there should be a Late Helladic artificial channel crossing the Pheneos Polje in order to control the Aroanius River and prevent it from flooding the southern and eastern plain. He hypothesizes extensive Mycenaean hydro-engineering constructions according to which our coring spot would be located in a polder area that was subject to controlled flooding and could otherwise be used for agricultural purposes, as it is used today. However, such constructions have never been proven by archaeological excavations, and we do not see any clear evidence for such extensive human activity in our sediment record. A human influence on the shift in the geochemical proxies (PC1, Ca/Ti, Fe, C/N) around 3300 cal BP in Pheneos cannot be confirmed, as archaeological evidence is lacking. As the proxy signal is contemporaneous to changes in Kaisari and other records from the region, we conclude that it more likely reflects a climatic drying event around 3200 cal BP. However, due to the immanent age uncertainties, we are not able to contribute to the debate on narrowing down when exactly that period started.

5.2.3 Classical–Hellenistic to Medieval period (2429–490 cal BP)

Climate reconstruction for the last 2400 years is challenging in the four archives, as we see strong human impact and desiccation processes that additionally affect the geochemical proxies (Seguin et al., 2019; Unkel et al., 2014).

Overall, increasingly dry conditions seem to prevail in the area. During the last 2800 years, the sediment structure of PHE1 looks more similar to KES2; carbonate nodules are absent and high TOC/TN values of 21.6 around 2700 cal BP (150 cm) show that the eastern Pheneos Bay received more terrestrial influence. We assume that for several centuries the eastern Pheneos Bay was shaped by relatively dry conditions and was not covered by a considerably deep lake, but most likely regularly fell dry periodically. This is further supported by stronger oxidizing conditions and high variation in Ca content, notably in unit 7, reflecting the alternation between well-waterlogged and relatively dry environmental conditions. An alternative explanation for the variability in carbonates could be the agricultural use of the area during the Classical–Hellenistic and Roman periods (2429–1650 cal BP), but clear archaeological evidence for that is lacking. This pattern can be interpreted as a lasting transformation in the valley ecosystem starting around 3000 cal BP. The Ca peaks hereby suggest dry phases with strong authigenic carbonate precipitation, but due to age uncertainties and potential reworking of the material in this period, we cannot link the peaks to any specific drought periods.

During the Classical–Hellenistic periods around 2200 cal BP, the Asea record starts to be influenced by pedogenic processes and the occurrence of carbonate nodules, which may indicate desiccation (Unkel et al., 2014). At the same time, Lake Lerna experiences its driest phase (Katrantsiotis et al., 2019). Stymphalia and Kaisari show more stable conditions during this phase. For Kaisari, the PC1 proxy indicates slightly wetter conditions between 2200–1700 cal BP, a phase often referred to as part of the Roman Warm Period (RWP; Luterbacher et al., 2012), which is in agreement with other proxies from the region (Boyd, 2015; Finné et al., 2014; Weiberg et al., 2016).

In the eastern Mediterranean, these trends are also reflected in the modelling approach by Finné et al. (2019) and the records used therein (Fig. 8k). The Dark Ages Cold Period or Late Antique Little Ice Age period (ca. 1550–1200 BP; Büntgen et al., 2016; Helama et al., 2017), prominent in the Stymphalia record around 1200 cal BP by high variation in water availability (Seguin et al., 2019), is hardly visible in Pheneos and Kaisari. Pheneos and Kaisari, however, show a short phase with moderately wetter conditions from 1050 to 850 cal BP, which is in agreement with Gialova Lagoon (Fig. 8e; Katrantsiotis et al., 2018) and Closani Cave (Fig. 8j; Warken et al., 2018).

Historical sources report the existence of a large lake in Pheneos in 1895 CE, which was completely dried up by 1901 CE (Knauss, 1990). These strong changes cannot be observed in the sediment sequence, as the poljes have been completely drained and used for agricultural purposes since the 1930s CE. Hence, the uppermost 46–50 cm in the Pheneos and Kaisari cores shows signs of ploughing (Figs. 3, 4, Tables S1, S2), and the palaeoenvironmental signals for the last ca. 700 years have been destroyed.

The rocky, barren beach and palaeoshorelines (Fig. 2b) on the flanks in the southern part of the Pheneos basin point towards higher lake level stands at some point in the recent past. Their exact age is unknown, but in combination with the historically reported high stand in 1821–1834 CE, due to the destruction of all *katavothre* by the retreating Turkish troops (Knauss, 1990), the absence of rock coatings on the boulders, and the sparse vegetation around them, we may assume that they were formed during that short period. Yet, Pausanias, travelling through Greece in the 2nd century CE, already mentioned the existence of "mountains marks up to which, it is said, the water rose" (Paus. 8.14.1), which suggests that the existence of shorelines could also be older than expected. A closer investigation of these features is needed to give more precise information on their formation.

Research to better understand soil development and erosion processes in the research area is crucial to understand landscape development with respect to the increasing anthropogenic land use. Decreasing the age uncertainties in the chronologies, e.g. by finding datable organic macroremains or independent age markers, would facilitate the study of socio-environmental interactions. Further studies on the transformation of the landscape and land-use activities would additionally call for pollen analysis, although pollen preservation is extremely low (Walsh et al., 2017) or sometimes non-existent as the authors' own (unpublished) test samples from Stymphalia have shown.

6 Conclusions

Our comparative analysis of PC1 proxy responses between neighbouring lakes improved the palaeoclimatic interpretation compared to single-site studies such as Stymphalia and Asea. Based on the geochemical analysis of the four study sites, we identified different phases when permanent lake water bodies existed at all sites (ca. 5000–3600 cal BP), as well as phases when the lakes episodically or at least seasonally dried out (around 3200 cal BP or during the last 1000 years), contributing to closing a gap in the understanding of water availability in the northern and central Peloponnese during culturally important periods. Our analyses show that Kaisari has never been a deep permanent lake over the last 5000 years, but regularly dried out. Due to its small size and the comparatively homogeneous catchment, it seems not very suitable as a high-resolution palaeoenvironmental archive. In Pheneos, phases with a more permanent lake water body were identified for the Mid-Holocene (5100–3600 cal BP), while the Late Holocene was likewise characterized by regular desiccation. There is an indication of a shift towards drier conditions around 3000 cal BP in the Pheneos and Kaisari records; however, due to dating uncertainties, especially in the Pheneos record, there is a high uncertainty in the exact timing of this dry period. On the other hand, according to the Stymphalia record, the main drying trend started after 2800 cal BP, culminating at around 2200 cal BP, which is in accordance with other records from the Peloponnese (Fig. 8a, e, f). Human impact cannot be excluded as an alternative explanation, as this falls into the time of the Late Helladic period with intensifying human activity, but this requires more archaeological evidence in combination with palaeoenvironmental investigations. We did not see any dramatic shift in the proxies, which would hint towards rapid climatic changes with a severe impact on the human population, but we rather noticed gradual variations. We thus suggest that climatic changes may have been only one factor in a multi-causal interaction network that contributed to but did not cause social transformations, contrasting the hypothesis of a climate-induced Late Bronze Age collapse (Drake, 2012).

Another plausible hypothesis would be that these basins integrate the climate signal over the catchment and thus may be less useful to pick up short-term variation in the way they are recorded in speleothems (Finné et al., 2014, 2017).

Interpreting proxy records on different spatial scales is promising to identify different, nested signals, which allows a more holistic understanding of landscape changes. Our study shows that geoarchives in mesoscale proximity to each other show similar trends and respond generally in a similar way to climate variations on the next larger scale. However, the mountainous landscape and the specific karst morphology of the Peloponnese cause a significant modulation in the response of the archives to climate, environmental, and human forcing on a local valley scale. The uncertainty ranges of the radiocarbon-based chronologies of more than 100 years, both in most geoarchives and in the archaeological record of the Peloponnese, as well as the difficulties of the assumption of an appropriate reservoir effect, inherent to the dating of bulk sediment samples, limit the extent to which conclusions on cause and effect within the interaction between humans and their environment can be drawn.

Data availability. Primary datasets for the sites Kaisari and Pheneos have been submitted to PANGAEA: https://doi.org/10.1594/PANGAEA.921425 (Seguin et al., 2020a) and https://doi.org/10.1594/PANGAEA.921424 (Seguin et al., 2020b).

Supplement. The supplement related to this article is available online at: https://doi.org/10.5194/egqsj-69-165-2020-supplement.

Author contributions. JS carried out the lab work, statistical analyses, and interpretation of the data. JS wrote the manuscript with contributions from all authors, above all from IU and TK. IU and AH are project investigators and designed the project. PA supported the sampling and field campaigns of Pheneos and Kaisari and contributed to the interpretations. TK and AH provided information on archaeological finds. AS contributed Asea data. All authors have read and approved the final version of the manuscript.

Competing interests. The authors declare that they have no conflict of interest.

Acknowledgements. We kindly thank the two reviewers for their valuable comments that helped to improve an earlier version of the manuscript. Furthermore, we thank our following colleagues and students for their invaluable support in the field: Dimitris Bassukas, Alexandros Emmanouilidis, Konstantinos Nikolaou, and Jan Weber. Sophia Dazert and McKenzie Elliott are acknowledged for support and assistance during laboratory work. Special thanks are due to Thomas Birndorfer, who was instrumental in creating the map in Fig. 1. The project was carried out with the relevant permits from

Greek authorities, the Institute of Geology and Mineral Exploration of Greece (IGME), and the Water Management Body of the Decentralized Prefecture of Peloponnese, Western Greece and the Ionian Islands.

Financial support. This research has been supported by the Collaborative Research Centre 1266 "Scales of Transformation – Human-environmental interaction in prehistoric and archaic societies" of the German Research foundation (DFG, project number 2901391021).

Review statement. This paper was edited by Elisabeth Dietze and reviewed by two anonymous referees.

References

Aitchison, J. and Greenacre, M.: Biplots of compositional data, J. R. Stat. Soc. C-Appl., 51, 375–392, https://doi.org/10.1111/1467-9876.00275, 2002.

Atherden, M. and Hall, J. A.: Holocene pollen diagrams from Greece, Hist. Biol., 9, 117–130, https://doi.org/10.1080/10292389409380493, 1994.

Bini, M., Zanchetta, G., Perşoiu, A., Cartier, R., Català, A., Cacho, I., Dean, J. R., Di Rita, F., Drysdale, R. N., Finnè, M., Isola, I., Jalali, B., Lirer, F., Magri, D., Masi, A., Marks, L., Mercuri, A. M., Peyron, O., Sadori, L., Sicre, M.-A., Welc, F., Zielhofer, C., and Brisset, E.: The 4.2 ka BP Event in the Mediterranean region: an overview, Clim. Past, 15, 555–577, https://doi.org/10.5194/cp-15-555-2019, 2019.

Bintliff, J. L.: The Complete Archaeology of Greece, from Hunter-Gatherers to the Twentieth Century AD, Blackwell-Wiley, Oxford, UK, New York, USA, 2012.

Blaauw, M. and Christeny, J. A.: Flexible paleoclimate age-depth models using an autoregressive gamma process, Bayesian Anal., 6, 457–474, https://doi.org/10.1214/11-BA618, 2011.

Boyd, M.: Speleothems in Warm Climates?: Holocene records from the Caribbean and Mediterranean. Dissertation, Stockholm University, Stockholm, Sweden, 2015.

Büntgen, U., Myglan, V. S., Ljungqvist, F. C., Mccormick, M., Cosmo, N. Di, Sigl, M., Jungclaus, J., Wagner, S., Krusic, P. J., Esper, J., Kaplan, J. O., Vaan, M. A. C. De, Luterbacher, J., Wacker, L., Tegel, W., and Kirdyanov, A. V.: Cooling and societal change during the Late Antique Little Ice Age from 536 to around 660 AD, Nat. Geosci., 9, 231–237, https://doi.org/10.1038/NGEO2652, 2016.

Croudace, I. W. and Rothwell, R. G.: Micro-XRF Studies of Sediment Cores, edited by: Croudace, I. W. and Rothwell, R. G., Springer Netherlands, Dordrecht, the Netherlands, 2015.

Drake, B. L.: The influence of climatic change on the Late Bronze Age Collapse and the Greek Dark Ages, J. Archaeol. Sci., 39, 1862–1870, https://doi.org/10.1016/j.jas.2012.01.029, 2012.

Dypvik, H. and Harris, N. B.: Geochemical facies analysis of fine-grained siliciclastics using Th/U, Zr/Rb and (Zr + Rb)/Sr ratios, Chem. Geol., 181, 131–146, https://doi.org/10.1016/S0009-2541(01)00278-9, 2001.

Emmanouilidis, A., Katrantsiotis, C., Norström, E., Risberg, J., Kylander, M., Sheik, T. A., Iliopoulos, G., and Avramidis, P.: Middle to late Holocene palaeoenvironmental study of Gialova Lagoon, SW Peloponnese, Greece, Quatern. Int., 476, 46–62, https://doi.org/10.1016/j.quaint.2018.03.005, 2018.

Emmanouilidis, A., Unkel, I., Triantaphyllou, M., and Avramidis, P.: Late-Holocene coastal depositional environments and climate changes in the Gulf of Corinth, Greece, Holocene, 30, 77–89, https://doi.org/10.1177/0959683619875793, 2019.

Erath, G.: Archäologische Funde im Becken von Pheneos, in: Pheneos und Lousoi. Untersuchungen zu Geschichte und Topographie Nordostarkadiens, edited by: Tausend, K., Frankfurt am Main, Germany, 199–237, 1999.

Finné, M., Holmgren, K., Sundqvist, H. S., Weiberg, E., and Lindblom, M.: Climate in the eastern Mediterranean, and adjacent regions, during the past 6000 years – A review, J. Archaeol. Sci., 38, 3153–3173, https://doi.org/10.1016/j.jas.2011.05.007, 2011.

Finné, M., Bar-Matthews, M., Holmgren, K., Sundqvist, H. S., Liakopoulos, I., and Zhang, Q.: Speleothem evidence for late Holocene climate variability and floods in Southern Greece, Quaternary Res., 81, 213–227, https://doi.org/10.1016/j.yqres.2013.12.009, 2014.

Finné, M., Holmgren, K., Shen, C.-C., Hu, H.-M., Boyd, M., and Stocker, S.: Late Bronze Age climate change and the destruction of the Mycenaean Palace of Nestor at Pylos, edited by J. P. Hart, PLoS One, 12, e0189447, https://doi.org/10.1371/journal.pone.0189447, 2017.

Finné, M., Woodbridge, J., Labuhn, I., and Roberts, C. N.: Holocene hydro-climatic variability in the Mediterranean: A synthetic multi-proxy reconstruction, Holocene, 29, 847–863, https://doi.org/10.1177/0959683619826634, 2019.

Forsén, J. and Forsén, B.: The Asea Valley Survey. An Arcadian Mountain Valley from the Palaeolithic Period until Modern Times, Paul Åströms Förlag, Stockholm, Sweden, 2003.

Gogou, A., Triantaphyllou, M., Xoplaki, E., Izdebski, A., Parinos, C., Dimiza, M., Bouloubassi, I., Luterbacher, J., Kouli, K., Martrat, B., Toreti, A., Fleitmann, D., Rousakis, G., Kaberi, H., Athanasiou, M., and Lykousis, V.: Climate variability and socio-environmental changes in the northern Aegean (NE Mediterranean) during the last 1500 years, Quaternary Sci. Rev., 136, 209–228, https://doi.org/10.1016/j.quascirev.2016.01.009, 2016.

Grimm, E. C., Maher, L. J., and Nelson, D. M.: The magnitude of error in conventional bulk-sediment radiocarbon dates from central North America, Quaternary Res., 72, 301–308, https://doi.org/10.1016/j.yqres.2009.05.006, 2009.

Grootes, P. M., Nadeau, M.-J., and Rieck, A.: 14C-AMS at the Leibniz-Labor: radiometric dating and isotope research, Nucl. Instrum. Meth. B, 223–224, 55–61, https://doi.org/10.1016/j.nimb.2004.04.015, 2004.

Helama, S., Jones, P. D., and Briffa, K. R.: Dark Ages Cold Period: A literature review and directions for future research, Holocene, 27, 1600–1606, https://doi.org/10.1177/0959683617693898, 2017.

Heymann, C., Nelle, O., Dörfler, W., Zagana, H., Nowaczyk, N., Xue, J., and Unkel, I.: Late Glacial to mid-Holocene palaeoclimate development of southern Greece inferred from the sediment sequence of Lake Stymphalia (NE-Peloponnese), Quatern. Int., 302, 42–60, https://doi.org/10.1016/j.quaint.2013.02.014, 2013.

Howell, R.: A Survey of Eastern Arcadia in Prehistory, Annu. Br. Sch. Athens, 65, 79–127, https://doi.org/10.1017/S0068245400014702, 1970.

Institute of Geology and Mineral Exploration of Greece (IGME): Geological Map of Greece, 1 : 50 000 (Sheet Nemea), Athens, Greece, 1970.

Institute of Geology and Mineral Exploration of Greece (IGME): Geological Map of Greece, 1 : 50 000 (Sheet Kandila), Athens, Greece, 1982.

Institute of Geology and Mineral Exploration of Greece (IGME): Geological Map of Greece, 1 : 50 000 (Sheet Megalopolis), Athens, Greece, 1992.

Institute of Geology and Mineral Exploration of Greece (IGME): Geological Map of Greece, 1 : 50 000 (Sheet Kollinai), Athens, Greece, 2002.

Isola, I., Zanchetta, G., Drysdale, R. N., Regattieri, E., Bini, M., Bajo, P., Hellstrom, J. C., Baneschi, I., Lionello, P., Woodhead, J., and Greig, A.: The 4.2 ka event in the central Mediterranean: new data from a Corchia speleothem (Apuan Alps, central Italy), Clim. Past, 15, 135–151, https://doi.org/10.5194/cp-15-135-2019, 2019.

Izdebski, A., Pickett, J., Roberts, N., and Waliszewski, T.: The environmental, archaeological and historical evidence for regional climatic changes and their societal impacts in the Eastern Mediterranean in Late Antiquity, Quaternary Sci. Rev., 136, 189–208, https://doi.org/10.1016/j.quascirev.2015.07.022, 2016.

Jahns, S.: On the Holocene vegetation history of the Argive Plain (Peloponnese, southern Greece), Veg. Hist. Archaeobot., 2, 187–203, https://doi.org/10.1007/bf00198161, 1993.

Kaniewski, D., Van Campo, E., Guiot, J., Le Burel, S., Otto, T., and Baeteman, C.: Environmental Roots of the Late Bronze Age Crisis, PLoS One, 8, 1–10, https://doi.org/10.1371/journal.pone.0071004, 2013.

Kaniewski, D., Marriner, N., Cheddadi, R., Guiot, J., and Van Campo, E.: The 4.2 ka BP event in the Levant, Clim. Past, 14, 1529–1542, https://doi.org/10.5194/cp-14-1529-2018, 2018.

Katrantsiotis, C., Norstro m, E., Holmgren, K., Risberg, J., and Skelton, A.: High-resolution environmental reconstruction in SW Peloponnese, Greece, covering around the last c. 6000 years: Evidence from Agios Floros fen, Messenian plain, Holocene, 26, 188–204, https://doi.org/10.1177/0959683615596838, 2015.

Katrantsiotis, C., Kylander, M. E., Smittenberg, R. H., Yamoah, K. K. A., Hättestrand, M., Avramidis, P., Strandberg, N. A., and Norström, E.: Eastern Mediterranean hydroclimate reconstruction over the last 3600 years based on sedimentary n-alkanes, their carbon and hydrogen isotope composition and XRF data from the Gialova Lagoon, SW Greece, Quaternary Sci. Rev., 194, 77–93, https://doi.org/10.1016/j.quascirev.2018.07.008, 2018.

Katrantsiotis, C., Norström, E., Smittenberg, R. H., and Finne, M.: Climate changes in the Eastern Mediterranean over the last 5000 years and their links to the high-latitude atmospheric patterns and Asian monsoons, Global Planet. Change, 175, 36–51, https://doi.org/10.1016/j.gloplacha.2019.02.001, 2019.

Knapp, A. B. and Manning, S. W.: Crisis in Context: The End of the Late Bronze Age in the Eastern Mediterranean, Am. J. Archaeol. 120, 99–149, https://doi.org/10.3764/aja.120.1.0099, 2016.

Knauss, J.: Der Graben des Herakles im Becken von Pheneos und die Vertreibung der stymphalischen Vögel, Athenische Mitteilungen, 105, 1–52, 1990.

Knitter, D., Hamer, W., Günther, G., Seguin, J., Unkel, I., Kessler, T., Weiberg, E., Duttmann, R., and Nakoinz, O.: Land use patterns and climate change – a modeled scenario of Late Bronze Age in Southern Greece, Environ. Res. Lett., 14, 125003, https://doi.org/10.1088/1748-9326/ab5126, 2019.

Kylander, M. E., Ampel, L., Wohlfarth, B., and Veres, D.: High-resolution X-ray fluorescence core scanning analysis of Les Echets (France) sedimentary sequence: new insights from chemical proxies, J. Quaternary Sci., 26, 109–117, https://doi.org/10.1002/jqs.1438, 2011.

Lauer, W. and Bendix, J.: Klimatologie. Das geographische Seminar, 2, Westermann, Braunschweig, Germany, 2006.

Lolos, Y. A.: Land of Sikyon. Archaeology and History of a Greek City-state, American School of Classical Studies at Athens, Princeton, NJ, USA, 2011.

Luterbacher, J., García-Herrera, R., Akcer-On, S., Allan, R., Alvarez-Castro, M.-C., Benito, G., Booth, J., Büntgen, U., Cagatay, N., Colombaroli, D., Davis, B., Esper, J., Felis, T., Fleitmann, D., Frank, D., Gallego, D., Garcia-Bustamante, E., Glaser, R., Gonzalez-Rouco, F. J., Goosse, H., Kiefer, T., Macklin, M. G., Manning, S. W., Montagna, P., Newman, L., Power, M. J., Rath, V., Ribera, P., Riemann, D., Roberts, N., Sicre, M.-A., Silenzi, S., Tinner, W., Tzedakis, P. C., Valero-Garcés, B., van der Schrier, G., Vannière, B., Vogt, S., Wanner, H., Werner, J. P., Willett, G., Williams, M. H., Xoplaki, E., Zerefos, C. S., and Zorita, E.: A Review of 2000 Years of Paleoclimatic Evidence in the Mediterranean, in: The Climate of the Mediterranean Region, edited by: Lionello, P., Elsevier, 87–185, https://doi.org/10.1016/C2011-0-06210-5, 2012.

Manning, S. W.: Chronology and terminology, in: The Oxford Handbook of the Bronze Age Aegean (Ca. 3000–1000 BC), edited by: Cline, E. H., Oxford University Press, Oxford, UK, 11–28, 2010.

Masi, A., Francke, A., Pepe, C., Thienemann, M., Wagner, B., and Sadori, L.: Vegetation history and paleoclimate at Lake Dojran (FYROM/Greece) during the Late Glacial and Holocene, Clim. Past, 14, 351–367, https://doi.org/10.5194/cp-14-351-2018, 2018.

Mayewski, P. A., Rohling, E. E., Curt Stager, J., Karlén, W., Maasch, K. A., Meeker, L. D., Meyerson, E. A., Gasse, F., van Kreveld, S., Holmgren, K., Lee-Thorp, J., Rosqvist, G., Rack, F., Staubwasser, M., Schneider, R. R., and Steig, E. J.: Holocene Climate Variability, Quaternary Res., 62, 243–255, https://doi.org/10.1016/j.yqres.2004.07.001, 2004.

McCormick, M., Büntgen, U., Cane, M. A., Cook, E. R., Harper, K., Huybers, P., Litt, T., Manning, S. W., Mayewski, P. A., More, A. F. M., Nicolussi, K., and Tegel, W.: Climate change during and after the roman Empire: reconstructing the past from scientific and historical evidence. J. Interdiscip. Hist., 43, 169–220, https://doi.org/10.1162/JINH_a_00379, 2012.

Meyers, P. A.: Applications of organic geochemistry to paleolimnological reconstructions: A summary of examples from the Laurentian Great Lakes, Org. Geochem., 34, 261–289, https://doi.org/10.1016/S0146-6380(02)00168-7, 2003.

Meyers, P. A. and Ishiwatari, R.: Lacustrine organic geochemistry-an overview of indicators of organic matter sources and diagenesis in lake sediments, Org. Geochem., 20, 867–900, https://doi.org/10.1016/0146-6380(93)90100-P, 1993.

Meyers, P. A. and Lallier-Vergès, E.: Lacustrine sedimentary organic matter records of Late Quaternary paleoclimates, J. Paleolimnol., 21, 345–372, 1999.

Mook, W. G. and van der Plicht, J.: Reporting 14C activities and concentrations, Radiocarbon, 41, 227–239, https://doi.org/10.1017/S0033822200057106, 1999.

Morfis, A. and Zojer, H.: Karst Hydrogeology of the Central and Eastern Peloponnesus (Greece), Steir. Beitr. zur Hydrogeol., 37/38, 1–301, 1986.

Munsell, A. H.: Munsell Soil Color Charts, Munsell Color, Grand Rapids, Michigan, USA, 2000.

Murray, M. R.: Is laser particle size determination possible for carbonate-rich lake sediments?, J. Paleolimnol., 27, 173–183, https://doi.org/10.1023/A:1014281412035, 2002.

Nanou, E.-A. and Zagana, E.: Groundwater Vulnerability to Pollution Map for Karst Aquifer Protection (Ziria Karst System, Southern Greece), Geosciences, 8, 125, https://doi.org/10.3390/geosciences8040125, 2018.

Neugebauer, I., Brauer, A., Schwab, M. J., Dulski, P., Frank, U., Hadzhiivanova, E., Kitagawa, H., Litt, T., Schiebel, V., Taha, N., and Waldmann, N. D.: Evidences for centennial dry periods at ∼ 3300 and ∼ 2800 cal. yr BP from micro-facies analyses of the Dead Sea sediments, Holocene, 25, 1358–1371, https://doi.org/10.1177/0959683615584208, 2015.

Norström, E., Katrantsiotis, C., Finné, M., Risberg, J., Smittenberg, R. H., and Bjursäter, S.: Biomarker hydrogen isotope composition (δD) as proxy for Holocene hydroclimatic change and seismic activity in SW Peloponnese, Greece, J. Quaternary. Sci., 33, 563–574, https://doi.org/10.1002/jqs.3036, 2018.

Olsson, I. U.: Accuracy and precision in sediment chronology, Hydrobiologia, 214, 25–34, https://doi.org/10.1007/BF00050928, 1991.

Psomiadis, D., Dotsika, E., Albanakis, K., Ghaleb, B., and Hillaire-Marcel, C.: Speleothem record of climatic changes in the northern Aegean region (Greece) from the Bronze Age to the collapse of the Roman Empire, Palaeogeogr. Palaeocl., 489, 272–283, https://doi.org/10.1016/j.palaeo.2017.10.021, 2018.

Ramisch, A., Tjallingii, R., Hartmann, K., Diekmann, B., and Brauer, A.: Echo of the Younger Dryas in Holocene Lake Sediments on the Tibetan Plateau, Geophys. Res. Lett., 45, 11154–11163, https://doi.org/10.1029/2018GL080225, 2018.

R Core Team: R: A language and environment for statistical computing, R Foundation for Statistical Computing, Vienna, Austria, available from: https://www.r-project.org/ (last access: 30 June 2020), 2019.

Reimer, P. J., Baillie, M. G. L., Bard, E., Bayliss, A., Beck, J. W., Blackwell, P. G., Bronk Ramsey, C., Buck, C. E., Burr, G. S., Edwards, R. L., Friedrich, M., Grootes, P. M., Guilderson, T. P., Hajdas, I., Heaton, T. J., Hogg, A. G., Hughen, K. A., Kaiser, K. F., Kromer, B., McCormac, F. G., Manning, S. W., Reimer, R. W., Richards, D. A., Southon, J. R., Talamo, S., Turney, C. S. M., van der Plicht, J., and Weyhenmeyer, C. E.: IntCal09 and Marine09 Radiocarbon Age Calibration Curves, 0–50 000 Years cal BP, Radiocarbon, 51, 1111–1150, https://doi.org/10.1017/S0033822200034202, 2009.

Reimer, P. J., Bard, E., Bayliss, A., Beck, J. W., Blackwell, P. G., Bronk Ramsey, C., Buck, C. E., Cheng, H., Edwards, R. L., Friedrich, M., Grootes, P. M., Guilderson, T. P., Haflidason, H., Hajdas, I., Hatté, C., Heaton, T. J., Hoffmann, D. L., Hogg, A. G., Hughen, K. A., Kaiser, K. F., Kromer, B., Manning, S. W., Niu, M., Reimer, R. W., Richards, D. A., Scott, E. M., Southon, J. R., Staff, R. A., Turney, C. S. M., and van der Plicht, J.: IntCal13 and Marine13 Radiocarbon Age Calibration Curves 0–50 ,000 Years cal BP, Radiocarbon, 55, 1869–1887, https://doi.org/10.2458/azu_js_rc.55.16947, 2013.

Richter, T. O., Van Der Gaast, S., Koster, B., Vaars, A., Gieles, R., De Stigter, H. C., De Haas, H., and Van Weering, T. C. E.: The Avaatech XRF Core Scanner: Technical description and applications to NE Atlantic sediments, Geol. Soc. Spec. Publ., 267, 39–50, https://doi.org/10.1144/GSL.SP.2006.267.01.03, 2006.

Roberts, N., Jones, M. D., Benkaddour, A., Eastwood, W. J., Filippi, M. L., Frogley, M. R., Lamb, H. F., Leng, M. J., Reed, J. M., Stein, M., Stevens, L., Valero-Garcés, B. L., and Zanchetta, G.: Stable isotope records of Late Quaternary climate and hydrology from Mediterranean lakes: the ISOMED synthesis, Quaternary Sci. Rev., 27, 2426–2441, https://doi.org/10.1016/j.quascirev.2008.09.005, 2008.

Roberts, N., Eastwood, W. J., Kuzucuoğlu, C., Fiorentino, G., and Caracuta, V.: Climatic, vegetation and cultural change in the eastern Mediterranean during the mid-Holocene environmental transition, Holocene, 21, 147–162, https://doi.org/10.1177/0959683610386819, 2011.

Roberts, N., Allcock, S. L., Arnaud, F., Dean, J. R., Eastwood, W. J., Jones, M. D., Leng, M. J., Metcalfe, S. E., Malet, E., Woodbridge, J., and Yiğitbaşıoğlu, H.: A tale of two lakes: a multiproxy comparison of Lateglacial and Holocene environmental change in Cappadocia, Turkey, J. Quaternary Sci., 31, 348–362, https://doi.org/10.1002/jqs.2852, 2016.

Rothacker, L., Dosseto, A., Francke, A., Chivas, A. R., Vigier, N., Kotarba-Morley, A. M., and Menozzi, D.: Impact of climate change and human activity on soil landscapes over the past 12 300 years, Sci. Rep., 8, 247, https://doi.org/10.1038/s41598-017-18603-4, 2018.

Sadori, L., Jahns, S., and Peyron, O.: Mid-Holocene vegetation history of the central Mediterranean, Holocene, 21, 117–129, https://doi.org/10.1177/0959683610377530, 2011.

Seguin, J., Bintliff, J. L., Grootes, P. M., Bauersachs, T., Dörfler, W., Heymann, C., Manning, S. W., Müller, S., Nadeau, M.-J., Nelle, O., Steier, P., Weber, J., Wild, E.-M., Zagana, E., and Unkel, I.: 2500 years of anthropogenic and climatic landscape transformation in the Stymphalia polje, Greece, Quaternary Sci. Rev., 213, 133–154, https://doi.org/10.1016/j.quascirev.2019.04.028, 2019.

Seguin, J., Avramidis, P., Haug, A., Kessler, T., Schimmelmann, A., and Unkel, I.: Geochemical and sedimentological record of sediment core KES2 retrieved from the Kaisari Polje (Peloponnese, Greece), PANGAEA, https://doi.org/10.1594/PANGAEA.921425, 2020a.

Seguin, J., Avramidis, P., Haug, A., Kessler, T., Schimmelmann, A., and Unkel, I.: Geochemical and sedimentological record of sediment core PHE1 retrieved from the Pheneos Polje (Peloponnese, Greece), PANGAEA, https://doi.org/10.1594/PANGAEA.921424, 2020b.

Stein, M., Migowski, C., Bookman, R., and Lazar, B.: Temporal changes in radiocarbon reservoir age in the dead sea-Lake Lisan system, Radiocarbon, 46, 649–655, https://doi.org/10.1017/S0033822200035700, 2004.

Tausend, K.: Die Siedlungen im Gebiet von Pheneos, in: Pheneos und Lousoi. Untersuchungen zu Geschichte und Topographie

Nordostarkadiens, edited by: Tausend, K., Frankfurt am Main, Germany, 331–342, 1999.

Triantaphyllou, M. V., Gogou, A., Dimiza, M. D., Kostopoulou, S., Parinos, C., Roussakis, G., Geraga, M., Bouloubassi, I., Fleitmann, D., Zervakis, V., Velaoras, D., Diamantopoulou, A., Sampatakaki, A., and Lykousis, V.: Holocene Climatic Optimum centennial-scale paleoceanography in the NE Aegean (Mediterranean Sea), Geo-Marine Lett., 36, 51–66, https://doi.org/10.1007/s00367-015-0426-2, 2016.

Unkel, I., Schimmelmann, A., Shriner, C., Forsén, J., Heymann, C., and Brückner, H.: The environmental history of the last 6500 years in the Asea Valley (Peloponnese, Greece) and its linkage to the local archaeological record, Z. Geomorphol. Supp., 58, 89–107, https://doi.org/10.1127/0372-8854/2014/S-00160, 2014.

Vaezi, A., Ghazban, F., Tavakoli, V., Routh, J., Beni, A. N., Bianchi, T. S., Curtis, J. H., and Kylin, H.: A Late Pleistocene-Holocene multi-proxy record of climate variability in the Jazmurian playa, southeastern Iran, Palaeogeogr. Palaeocl., 514, 754–767, https://doi.org/10.1016/j.palaeo.2018.09.026, 2019.

van Geel, B., Heijnis, H., Charman, D. J., Thompson, G., and Engels, S.: Bog burst in the eastern Netherlands triggered by the 2.8 kyr BP climate event, Holocene, 24, 1465–1477, https://doi.org/10.1177/0959683614544066, 2014.

Walker, M., Head, M. J., Lowe, J., Berkelhammer, M., BjÖrck, S., Cheng, H., Cwynar, L. C., Fisher, D., Gkinis, V., Long, A., Newnham, R., Rasmussen, S. O., and Weiss, H.: Subdividing the Holocene Series/Epoch: formalization of stages/ages and subseries/subepochs, and designation of GSSPs and auxiliary stratotypes, J. Quaternary Sci., 34, 173–186, https://doi.org/10.1002/jqs.3097, 2019.

Walsh, K., Brown, A. G., Gourley, B., and Scaife, R.: Archaeology, hydrogeology and geomythology in the Stymphalos valley, J. Archaeol. Sci. Rep., 15, 446–458, https://doi.org/10.1016/j.jasrep.2017.03.058, 2017.

Walsh, K., Berger, J.-F., Roberts, N., Vannière, B., Ghilardi, M., Brown, A. G., Woodbridge, J., Lespez, L., Estrany, J., Glais, A., Palmisano, A., Finné, M., Verstraeten, G., Roberts, C. N., Vanniere, B., Ghilardi, M., Brown, A. G., Woodbridge, J., Lespez, L., Estrany, J., Glais, A., Palmisano, A., Finné, M., and Verstraeten, G.: Holocene demographic fluctuations, climate and erosion in the Mediterranean: A meta data-analysis, Holocene, 29, 864–885, https://doi.org/10.1177/0959683619826637, 2019.

Wanner, H.: Die angewandte Geländeklimatologie – ein aktuelles Arbeitsgebiet der physischen Geographie, Erdkunde, 40, 1–14, 1986.

Warken, S. F., Fohlmeister, J., Schröder-Ritzrau, A., Constantin, S., Spötl, C., Gerdes, A., Esper, J., Frank, N., Arps, J., Terente, M., Riechelmann, D. F. C., Mangini, A., and Scholz, D.: Reconstruction of late Holocene autumn/winter precipitation variability in SW Romania from a high-resolution speleothem trace element record, Earth Planet. Sc. Lett., 499, 122–133, https://doi.org/10.1016/j.epsl.2018.07.027, 2018.

Weiberg, E., Unkel, I., Kouli, K., Holmgren, K., Avramidis, P., Bonnier, A., Dibble, F., Finné, M., Izdebski, A., Katrantsiotis, C., Stocker, S. R., Andwinge, M., Baika, K., Boyd, M., and Heymann, C.: The socio-environmental history of the Peloponnese during the Holocene: Towards an integrated understanding of the past, Quaternary Sci. Rev., 136, 40–65, https://doi.org/10.1016/j.quascirev.2015.10.042, 2016.

Weiberg, E., Bevan, A., Kouli, K., Katsianis, M., Woodbridge, J., Bonnier, A., Engel, M., Finné, M., Fyfe, R., Maniatis, Y., Palmisano, A., Panajiotidis, S., Roberts, C. N., and Shennan, S.: Long-term trends of land use and demography in Greece: A comparative study, Holocene, 29, 742–760, https://doi.org/10.1177/0959683619826641, 2019.

Weltje, G. J. and Tjallingii, R.: Calibration of XRF core scanners for quantitative geochemical logging of sediment cores: Theory and application, Earth Planet. Sc. Lett., 274, 423–438, https://doi.org/10.1016/j.epsl.2008.07.054, 2008.

Weltje, G. J., Bloemsma, M. R., Tjallingii, R., Heslop, D., Röhl, U., and Croudace, I. W.: Prediction of Geochemical Composition from XRF Core Scanner Data: A New Multivariate Approach Including Automatic Selection of Calibration Samples and Quantification of Uncertainties, edited by: Croudace, I. W. and Rothwell, R. G., Springer Dordrecht, the Netherlands, 507–534, https://doi.org/10.1007/978-94-017-9849-5_21, 2015.

Williams, E. H.: Stymphalos: A Planned City of Ancient Arcadia, Echos du Monde Class. = Class. Views, 27, 194–205, 1983.

Williams, H.: Archaeological Investigations at Ancient Stymphalos, 1982–2008, in: The Corinthia and the Northeast Peloponnese. Topography and History from Prehistoric Times until the End of Antiquity, edited by: Kissas, K. and Niemeier, W. D., Munich, Germany, 425–431, 2013.

Williams, H. and Gourley, B.: The fortifications of Stymphalos, Mouseion: Journal of the Classical Association of Canada, 5, 213–225, 2005.

Xu, H., Liu, B., and Wu, F.: Spatial and temporal variations of Rb/Sr ratios of the bulk surface sediments in Lake Qinghai, Geochem. Trans., 11, 3, https://doi.org/10.1186/1467-4866-11-3, 2010.

Zanchetta, G., Sulpizio, R., Roberts, N., Cioni, R., Eastwood, W. J., Siani, G., Caron, B., Paterne, M., and Santacroce, R.: Tephrostratigraphy, chronology and climatic events of the Mediterranean basin during the Holocene: An overview, Holocene, 21, 33–52, https://doi.org/10.1177/0959683610377531, 2011.

Zanchetta, G., Regattieri, E., Isola, I., Drysdale, R. N., Bini, M., Baneschi, I., and Hellstrom, J. C.: The so-called "4.2 event" in the central Mediterranean and its climatic teleconnections, Alp. Mediterr. Quat., 29, 5–17, 2016.